Water Practice & Technology

IWA PUBLISHING

Water Practice & Technology Vol 18 No 12, 3065 doi: 10.2166/wpt.2023.214

A comprehensive review on the sequestration of dyes from aqueous media using maize-/corn-based adsorbents

Kingsley O. Iwuozor[a], Chisom T. Umeh[a], Stephen Sunday Emmanuel[b], Ebuka Chizitere Emenike[a,*], Abel U. Egbemhenghe[c], Odunayo T. Ore[d], Taiwo Temitayo Micheal[e], Fredrick O. Omoarukhe[f], Patience A. Sagboye[f], Victor E. Ojukwu[g] and Adewale George Adeniyi[f,h]

[a] Department of Pure and Industrial Chemistry, Nnamdi Azikiwe University, P. M. B. 5025, Awka, Nigeria
[b] Department of Industrial Chemistry, University of Ilorin, P. M. B. 1515, Ilorin, Nigeria
[c] Department of Chemistry, Lagos State University, Ojo, Lagos, Nigeria
[d] Department of Chemistry, Obafemi Awolowo University, Ile-Ife, Nigeria
[e] Department of Agricultural Engineering, Ladoke Akintola University of Technology, P. M. B. 4000, Ogbomosho, Nigeria
[f] Department of Chemical Engineering, University of Ilorin, P. M. B. 1515, Ilorin, Nigeria
[g] Department of Chemical Engineering, Nnamdi Azikiwe University, P. M. B. 5025, Awka, Nigeria
[h] Department of Chemical Engineering, Landmark University, P.M.B. 1001, Omu-Aran, Nigeria
*Corresponding author. E-mail: emenikechizitere@gmail.com

ECE, 0000-0001-7117-3265; PAS, 0009-0004-5674-4268

ABSTRACT

Corn or maize (*Zea mays* L.) is the most significant grain crop worldwide after wheat and rice. It is widely cultivated and consumed as food, feed, and industrial raw material, along with the emission of a large quantity of corn waste. Such abundant, renewable, and cheap wastes with unique chemical compositions can be efficiently converted into adsorbents for the elimination of dye-contaminated water. This article represents an extensive review of the use of corn/maize waste-derived adsorbents for the sequestration of dyes from aqueous media. This study addressed the utilization of corn residues, including cob, stalk, straw, husk, and silk, as precursors for adsorbents. The adsorption behaviour, mechanism, and regeneration of the studied corn adsorbent/dye systems were identified. It was observed that the most common forms of corn/maize-derived adsorbents that have been utilized for the sequestration of dyes include biosorbents, biochars, activated carbons, and composites. The highest adsorption capacity (1,682.7 mg/g) for dye (methylene blue) sequestration was obtained using a corn husk composite-based adsorbent. Important findings and future ideas are finally mentioned for the corn/maize-based materials and their application as adsorbents for dye removal.

Key words: adsorption, composite adsorbent, corn cob, dyes, environment

HIGHLIGHTS

- Use of corn adsorbents strengthens the popular waste-to-wealth management strategy.
- The adsorbent groups include biosorbents, activated carbons, biochar, and composites.
- Major mechanisms are electrostatic attraction, ion exchange, and hydrogen bonding.
- The adsorbents can be recycled and reused several times.
- The highest adsorption capacity (1,682.7 mg/g) was obtained using a corn husk-based composite.

GRAPHICAL ABSTRACT

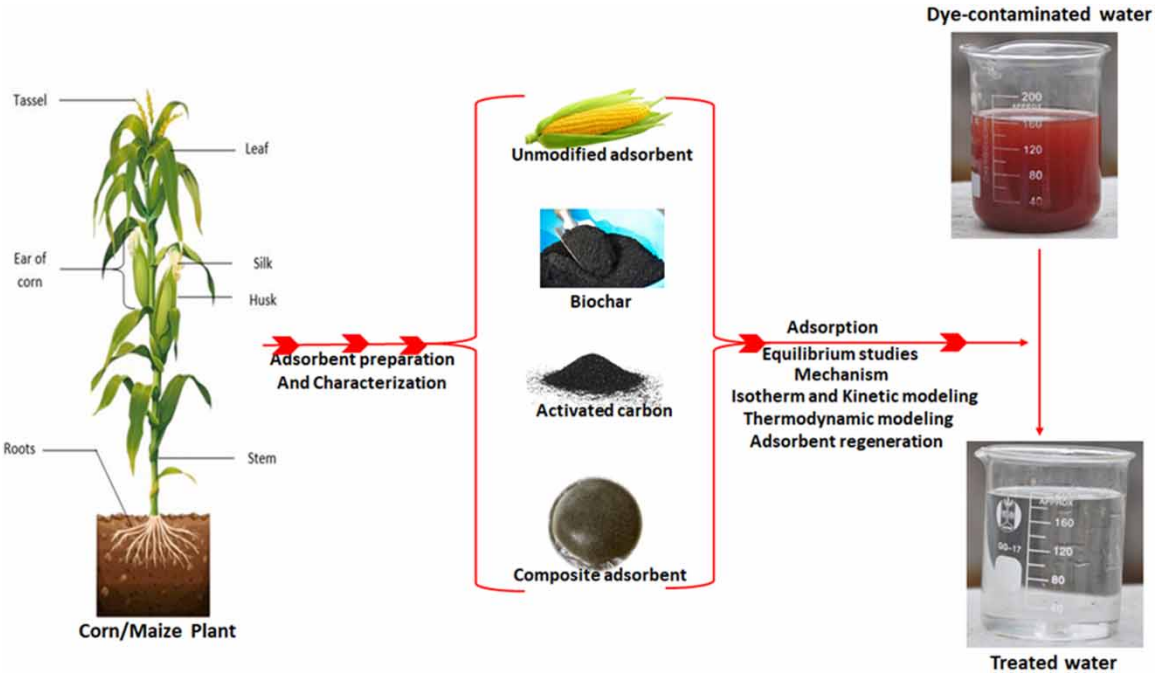

1. INTRODUCTION

The discharge of contaminants from agricultural, industrial, and municipal activities has a significant impact on public health and aquatic environments (Iwuozor *et al.* 2022a; Omuku *et al.* 2022). These contaminants include substances such as dyes, heavy metals, pesticides, pharmaceuticals, and phenolic compounds, among others (Zhul-quarnain *et al.* 2018; Adeniyi *et al.* 2022). Dyes are widely used in various industries such as textiles, leather, paper, and food, and their use has led to the release of substantial amounts of dye-containing wastewater into the environment (Abubakar & Batagarawa 2017; Abdullah *et al.* 2019). Dye contamination in the environment has become a significant environmental issue due to its toxicity, carcinogenicity, and mutagenicity (Yaneva & Georgieva 2013). These contaminants can have harmful impacts on the ecosystem, aquatic life, and human health. Dye contamination in the environment can affect water quality, leading to a decrease in oxygen levels and the accumulation of toxic substances that can result in the death of aquatic life (Abubakar & Batagarawa 2017; Ranjbar *et al.* 2022). Dye-contaminated water can also affect soil quality, leading to soil degradation, reduced crop productivity, and environmental pollution (Abdel-Aal *et al.* 2006; Zolgharnein *et al.* 2016; Ali *et al.* 2017). Conventional treatment methods for removing dyes from wastewater, such as physical, chemical, and biological techniques, have limitations and can be expensive. As a result, researchers have turned to alternative, cost-effective, and eco-friendly methods for the removal of dyes from aqueous media. Numerous methods have been developed to remove dyes from wastewater, such as adsorption, coagulation, and advanced oxidation processes (Balathanigaimani *et al.* 2009; Chen *et al.* 2011, 2020; Chang *et al.* 2021). Among these methods, adsorption has gained considerable attention as a simple, cost-effective, and efficient process (Abubakar & Batagarawa 2017; Ali *et al.* 2017). The use of adsorbents derived from natural materials, such as maize/corn-based adsorbents, has emerged as a promising approach for dye removal due to their abundance, low cost, and eco-friendly nature.

Corn or maize is a widely cultivated crop, and its by-products, including husks, cobs, stalks, and leaves, generate significant waste (Mu *et al.* 2020). These wastes are often left in the field, which can result in environmental issues such as soil degradation and pollution of water resources. In addition, the burning of corn waste in some regions can lead to air pollution and contribute to greenhouse gas emissions (Zheng *et al.* 2010; Zhao *et al.* 2014). In recent years, there has been a growing interest in utilizing corn waste as a sustainable and cost-effective solution to address these environmental issues. One promising approach is to convert corn waste into valuable products such as biofuels, biogas, and biodegradable plastics (Kamusoko *et al.* 2021). For instance, the fermentation of corn waste can produce biogas, which can be used as a renewable energy source for electricity generation

and heating. Maize/corn-based adsorbents have recently emerged as a promising alternative for the sequestration of dyes from aqueous media due to their abundance, low cost, renewability, and biodegradability (Rehl *et al.* 2012). These adsorbents have shown high adsorption capacities for various types of dyes, including synthetic and natural dyes, and have the potential to be used in large-scale wastewater treatment systems.

From the literature survey, it was found that there are a number of review articles that studied the application of corn/maize-based adsorbents for the treatment of water, but none of them were specific on the utilization of the adsorbents for the removal of dyes from aqueous media. For instance, the application of corn cob-based adsorbents for the treatment of heavy metals and dyes has been reviewed (Arquilada *et al.* 2018). Another study discussed the adsorption of specific aquatic pollutants, with a focus on heavy metals, by corn waste-based adsorbents (Sharma *et al.* 2019). Also, the pesticide adsorption on biochar derived from maize, rice, and wheat residues has been studied (Ogura *et al.* 2021). However, these reviews were specific and did not address the synthesis, properties, performance, and reusability of corn/maize-based adsorbents for dye sequestration in detail. This critical review aims to analyse the existing literature on the use of maize/corn-based adsorbents for the sequestration of dyes from aqueous media. This discusses the key aspects of adsorption processes, including adsorption mechanisms, adsorbent preparation, and the effect of various parameters such as pH, temperature, and contact time on the adsorption capacity. Furthermore, regeneration and reusability studies and competitive adsorption were discussed. Moreover, this review will also highlight the challenges and limitations of maize/corn-based adsorbents and identify future research directions to improve their efficiency. The review is restricted to only articles published in the literature in the past 10 years, and only articles published in English were considered.

2. PREPARATION OF MAIZE/CORN-BASED ADSORBENT

Owing to maize/corn's adequate obtainability and accessibility across many continents, their adsorbents have been researched for the elimination of umpteen pollutants from various aquatic environments. Furthermore, it is also worth noting that different maize organs are always disposed of as solid agro-waste, and thus, this has fuelled the attention of researchers in converting this type of agro-waste to an estimable value-added adsorbent, as this is seen as a way of strengthening from waste to wealth-health sustainability in general. For simplicity and lucidity, the discourse in the succeeding subheadings is structured with respect to the adsorbents' extensive classifications, viz., unmodified maize (UM), maize activated carbon (MAC), maize biochar (MBC), and maize composite (MC) adsorbent, as depicted in Figure 1.

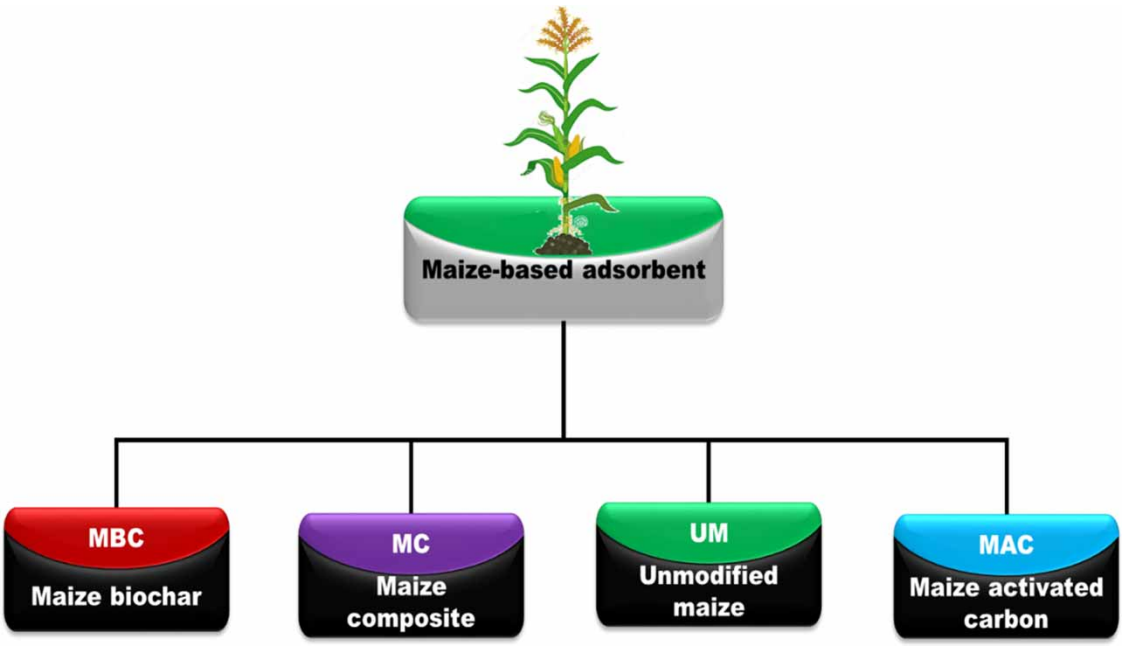

Figure 1 | Classification of maize-based adsorbents.

2.1. UM adsorbent/maize biosorbent

UM adsorbents are usually prepared by washing the as-collected maize matrix with H_2O to remove dirt, followed by drying under the shade, in sunlight, in an oven, or air-drying to remove or reduce its moisture and proliferate the active site's numerical strength for the adsorption process (Ponce *et al.* 2021). According to Petrović *et al.* (2017), the as-collected corn silk matrix obtained from planted corn was dried at 353 K, pulverized, and sieved to obtain <0.2 mm particle size. This preparation process was similar to the one carried out by Abubakar & Batagarawa (2017), Lima *et al.* (2018), Paşka *et al.* (2014), and Fadhil & Eisa (2019). However, Abubakar & Batagarawa (2017) sun dried their own maize organ (stalk) before oven drying at 65 °C for 24 h and then pounding and sieving to a mesh size of 106 μm, and this was somewhat similar to the water boiling of the plant matrix carried out by Dehvari *et al.* (2013) and Değermenci *et al.* (2019) before oven drying at 100 °C and 60 °C, respectively. The authors emphasized that the essence of boiling the plant samples mildly before proper drying is to improve adsorption. Conversely, Guyo *et al.* (2015) and Ibrahim (2013) air dried as-collected maize plant part samples after washing before pulverizing to the required size. Then, the maize plant sample needed to be cleansed using deionized water, dried once more to get rid of some impurities on its surface, and then sieved to obtain a smooth biosorbent with better porosity (Petrović *et al.* 2017).

2.2. Maize-based biochar

Biochar is a permeable pyrogenic carbonaceous material fabricated by thermal putrefaction of agricultural wastes such as maize cob, livestock mucks, and other biomass in an infinitesimal O_2 supply condition without any kind of chemical or physicochemical activation (Liu *et al.* 2018a; Billa *et al.* 2019; Eltaweil *et al.* 2020; Iwuozor *et al.* 2022b). According to Eltaweil *et al.* (2020), Iwuozor *et al.* (2022b), Yang *et al.* (2018), Wan *et al.* (2018), and Maneechakr & Karnjanakom (2019), this type of adsorbent fabrication approach is a revolutionary methodology that does not only help in reducing global warming that accompany the emission of CO_2 during open burning of biomass or biomass wastes but also afford the resulting adsorbent with excellent porous architecture, enhanced immunity to corrosion and degradation, availability of significant oxygen-containing organic architectural functional groups, and inexpensive fabrication budget, all of which render biochar as an eco-benign sorption candidate for the elimination or degradation of dye contaminants.

Accordingly, MBC is the product of maize matrix anoxic pyrolysis. From various reports gathered in Table 1, most of the authors (Ma *et al.* 2016; Gao *et al.* 2019; Tsamo *et al.* 2019; Li *et al.* 2019a, 2019b; Eltaweil *et al.* 2020; Mu *et al.* 2020; Zhang *et al.* 2020; Gao *et al.* 2021) prepared the MBC in a pyrolyzer/muffle furnace sustained between 300–800 °C for 120–360 min with a heating rate of 5–20 °C/min. In addition to the aforementioned harsh reactor condition, nitrogen gas is sometimes added to the biomass matrix in an effort to forefend ash formation as well as to maintain the inert environment in the pyrolyzer, owing to the fact that it has been experimentally established that the biochar yield and the explicit surface area profile are reliant on the aforementioned pyrolysis operating parameters (Gao *et al.* 2019; Ahmad *et al.* 2020; Zhang *et al.* 2020; Gao *et al.* 2021; Iwuozor *et al.* 2022b).

For instance, to prepare corn cob biochar, Zhang *et al.* (2020) first washed the collected cob with water and absolute EtOH. The biomass was then dried for 24 h in a vacuum chamber at 90 °C, followed by pulverizing and sieving to create fine char. The cob fine char was added to a corundum crucible, pyrolyzed under a nitrogen atmosphere for 2 h at a constant temperature of 600 °C (15 °C/min), and then chilled to ambient temperature while maintaining a nitrogen condition. The finished char was then grounded, neutralized with water and EtOH, and dried for 12 h at 90 °C. This similar method was adopted for the fabrication of nZVI/corn straw and functional corn straw biochar composites by Eltaweil *et al.* (2020) and Gao *et al.* (2021). Although, according to Eltaweil *et al.* (2020), the nZVI/corn straw composite was fabricated via a reduction process after the corn straw biochar had been successfully achieved, Gao *et al.* (2021) achieved the biochar composite in a single pyrolysis step. Shortly, as reported by Eltaweil *et al.* (2020), ethanol–water (EtOH-H_2O) (8:2 ml) was mixed with 50 mg of corn straw biochar and 180 mg of $FeCl_3.6H_2O$, and then the mixture was sonicated for 30 min. To convert Fe^{3+} ions into Fe^0, freshly made aqueous $NaBH_4$ was added in drops to the Fe^{3+}/corn straw composite blends. Following the complete addition of NaBH4, the magnetic nZVI/corn straw composite that emerged was detached with an external magnet, repeatedly rinsed with water and EtOH, and then dried overnight in an oven at 50 °C.

Table 1 | Summary of methodology for preparation of maize/corn adsorbents

		Modification/activation		Carbonization						
Plant parts	Adsorbent class	Reagent/material	Process	Temp (°C)	Heating rate (°C/min)	Time (mins)	Characterization	BET SSA (m^2/g)	Yield (wt %)	References
Cob	MAC	KOH	Base activation	800	–	1,440	FT-IR-ATR, SEM, XRD	–	–	Abdullah *et al.* (2019)
Cob	MC	Graphene oxide		60	–	120	FT-IR, SEM	–	–	Qu *et al.* (2020)
Cob	MB	–	–	60	–	–	–	–	–	Qu *et al.* (2020)
Cob	MAC	H_3PO_4	Acid activation	600	–	60	–	–	–	Ali *et al.* (2017)
Cob	MAC	H_3PO_4	Acid activation	600	–	60	–	–	–	Ali *et al.* (2017)
Cob	MAC	H_2SO_4	Acid activation	50	10	120	FT-IR, SEM	–	–	Aljeboree & Alkaim (2019)
Cob	MAC	H_3PO_4	Acid activation	5,000	–	60	FT-IR, SEM	–	–	Aljeboree *et al.* (2019)
Cob	MB	HCl	Pyrolysis + Acid activation	350	–	180	FT-IR, SEM, BET	–	–	Assirey & Altamimi (2021)
Cob	MB	HCl	Pyrolysis + Acid activation	450	–	180	FT-IR, SEM, BET	407	–	Assirey & Altamimi (2021)
Cob	MAC	H_3PO_4	Acid activation	500	0.2	60	FT-IR-ATR	–	–	Campos *et al.* (2020)
Stover	MAC	Ethanol-ammonia + aminopropyltriethoxysilane	–	70	–	960	FT-IR, XRD SEM-EDS, BET	0.693		Carijo *et al.* (2019)
Stalk	MAC	Epichlorohydroin and N,N-dimethylformamide and trimethylamine	–	100	–	1,440	–	–	–	Chen *et al.* (2012)
Straw pith	MAC	$ZnCl_2$	Salt activation	–	–	–	SEM, FT-IR, XRD	–	–	Chen *et al.* (2020)
Straw	MAC	KOH and NaOH	Pyrolysis + base activation	500	10	60	SEM, TEM, BET	1,993	–	Chen *et al.* (2019)
Stem	MAC	H_3PO_4, KOH, and ZnCl	Pyrolysis + acid, base and salt activation	–	–	–	–	–	25.8	Dada *et al.* (2012)
Starch	MAC	Hydrogen peroxide	Acid activation	80	–	60	SEM, FT-IR, XRD	–	–	Dai *et al.* (2017)
Silk	MB	–	–	60	–	4,320	SEM, FT-IR	–	–	Değermenci *et al.* (2019)
Tassel powder	MAC	–	–	102	–	144	UV-visible spectrophotometer	–	–	Dehvari *et al.* (2013)

(*Continued.*)

Table 1 | Continued

		Modification/activation		Carbonization						
Plant parts	Adsorbent class	Reagent/material	Process	Temp (°C)	Heating rate (°C/min)	Time (mins)	Characterization	BET SSA (m^2/g)	Yield (wt %)	References
Cob	MAC	$ZnCl_2$	Salt activation	500	–	60	BET, XRD, SEM, EDX, FT-IR	0.431	–	Dina *et al.* (2012)
Seed chaff	MB	–	–	100	–	300	FT-IR, SEM, EDX	–	–	Duru & Duru (2017)
Stalk	MB	–	–	100	–	300	FT-IR, SEM, EDX	–	–	Duru & Duru (2017)
Cob	MB	–	–	100	–	300	FT-IR, SEM, EDX	–	–	Duru & Duru (2017)
Husk	MB	–	–	100	–	300	FT-IR, SEM, EDX–	–	–	Duru & Duru (2017)
Husk	MAC	Tartaric acid	Pyrolysis + acid activation	100	–	240	EDXRF FT-IR	–	–	Duru *et al.* (2019)
Husk	MAC	Metanoic acid	Pyrolysis + acid activation	100	–	240	EDXRF, FT-IR	–	–	Duru *et al.* (2019)
Husk	MAC	Phenol	Pyrolysis + acid activation	100	–	240	EDXRF, FT-IR	–	–	Duru *et al.* (2019)
Cob	MAC	NaOH	Pyrolysis + base activation	500	–	120	XRD, Raman, FT-IR, TEM, EDS, XPS	–	–	Dutta & Nath (2018)
Cob	MAC	$AlCl_3$	Pyrolysis + acid activation	500	–	120	SEM, BET	146.64		El-Bendary *et al.* (2021)
Cob	MAC	–	Pyrolysis	500	–	120	SEM. BET	118.53		El-Bendary *et al.* (2021)
Cob	MAC	H_3PO_4	Acid activation + pyrolysis	400	–	120	BET	700		El-Sayed *et al.* (2014)
Cob	MAC	H_3PO_4	Acid activation + pyrolysis	500	–	120	BET	633		El-Sayed *et al.* (2014)
Cob	MAC	H_3PO_4	Acid activation + pyrolysis	600	–	120	BET	600		El-Sayed *et al.* (2014)
Straw	MBC	$FeCl_3.CH_2O$	Pyrolysis + acid activation	500	–	180	XRD, FT-IR, TEM-EDS, VSM, XPS, TGA, BET	80.1	–	Eltaweil *et al.* (2020)
Leaves	MAC	HCl	Acid activation	–	–	–	FT-IR, SEM	–	–	Fadhil & Eisa (2019)
Leaves	MAC	–	–	–	–	–	FT-IR, SEM	–	–	Fadhil & Eisa (2019)
Leaves	MAC	–	–	–	–	–	FT-IR, SEM	–	–	Fadhil *et al.* (2021)
Leaves	MAC	–	–	70	–	1,440	SEM	–	–	Fadhel *et al.* (2021)
Cob	MB	–	Pyrolysis	500	–	120	FT-IR, XRD, SEM	–	–	Farnane *et al.* (2018)

(*Continued.*)

Table 1 | Continued

Plant parts	Adsorbent class	Modification/activation		Carbonization			Characterization	BET SSA (m^2/g)	Yield (wt %)	References
		Reagent/material	Process	Temp (°C)	Heating rate (°C/min)	Time (mins)				
Cob	MAC	H_3PO_4	Pyrolysis + acid activation	500	–	120	FT-IR, XRD, SEM	–	–	Farnane *et al.* (2018)
Stalk	MAC	–	–	25	–	1,440	SEM, XRD, FT-IR	–	–	Fathi *et al.* (2015)
Cob	MB	–	–	–	–	–	–	–	–	Fatoye & Onigbinde (2020)
Straw	MBC	–	Pyrolysis	300	10	120	SEM, BET FT-IR	1.19	–	Gao *et al.* (2019)
Straw	MBC	–	Pyrolysis	800	10	120	SEM, BET FT-IR	74.33	–	Gao *et al.* (2019)
Straw + waste red mud	MBC	–	Pyrolysis	700	10	120	SEM, EDX, XRD, BET, XPS	20.34	–	Gao *et al.* (2021)
Hull	MAC	Tartaric acid	Acid activation	–	–	–	–	–	–	Ghasemi *et al.* (2017)
Straw	MAC	Succinic anhydride and xylene	Acid activation	–	–	–	FT-IR,SEM-EDX	–	–	Guo *et al.* (2015a)
Starch	MB	–	–	–	–	–	SEM, BET, BJH, pore size analyser	–	–	Guo *et al.* (2015b)
Porous starch	MAC	Sodium dihydrogen phosphate-citric acid buffer	Acid activation	–	–	–	SEM, BET, BJH, pore size analyser	–	–	Guo *et al.* (2015b)
Straw	MAC	Zinc acetate	Salt activation	–	–	–	SEM, XRD, FT-IR	–	–	Guo *et al.* (2018)
Straw	MAC	Zinc acetate and manganese acetate	Salt activation	–	–	–	SEM, XRD, FT-IR	–	–	Guo *et al.* (2018)
Straw	MB	–	–	–	–	–	SEM, XRD, FT-IR	–	–	Guo *et al.* (2018)
Stover	MB	–	–	–	–	–	–	–	–	Guyo *et al.* (2015)
Stover	MAC	HNO_3	Acid activation	–	–	–	–	–	–	Guyo *et al.* (2015)
Cob	MAC	–	–	–	–	–	–	–	–	Ibrahim (2013)
Stalk	MAC	HCl	Acid activation	–	–	–	–	–	–	Ismail *et al.* (2019)
Husk leaf	MAC	$Ca(OH)_2$	Salt activation	550	–	–	FT-IR, FE-SEM, XRF	–	–	Jalil *et al.* (2012)
Cob	MAC	–	–	100	–	1,200	FT-IR, SEM	–	–	Javed *et al.* (2021)
Cob	MAC	H_2SO_4	Acid activation	105	–	1,440	FT-IR, SEM, XRD, BET, CHNS-O	–	–	Jawad *et al.* (2018)
Straw	MB	–	–	–	–	–	BET, SEM, FT-IR	21.0	–	Jia & Li (2015)

(*Continued.*)

Table 1 | Continued

		Modification/activation		Carbonization						
Plant parts	Adsorbent class	Reagent/material	Process	Temp (°C)	Heating rate (°C/min)	Time (mins)	Characterization	BET SSA (m^2/g)	Yield (wt %)	References
Pith	MAC	H_2SO_4	Acid activation	–	–	–	BET, FT-IR, SEM, TGA, XRD	0.01	–	Jothirani *et al.* (2016)
Stalk + walnut shell	MAC	–	Pyrolysis	500	–	180	SEM, FT-IR, BET	1,187.00		Kang *et al.* (2018)
Husk	MAC	$ZnCl_2$	Salt activation	100	–	1,440	–	–	–	Khodaie *et al.* (2013)
Stalk	MAC	–	–	–	–	–	XRD, SEM-EDS, BET	4.79	–	Lara-Vásquez *et al.* (2016)
Cob	MAC	$ZnCl_2$	Salt activation	350	–	120	–	–	–	Leelavathy *et al.* (2015)
Cob	MAC	–	–	–	–	–	–	–	–	Leelavathy *et al.* (2015)
Stalk	MBC	Urea & $NaHCO_3$	Base activation + pyrolysis	700	10	120	BET, XRD, XPS	325.90	–	Li *et al.* (2019a)
Stalk	MAC	Ethyl acetate	Base activation	–	–	–	SEM, BET	201.0	–	Li *et al.* (2019b)
Straw	MB	–	–	–	–	–	FT-IR, XRD, SEM, BET	0.85	–	Lima *et al.* (2017)
Straw	MB	–	–	–	–	–	FT-IR, XRD, SEM, BET	0.85	–	Lima *et al.* (2018)
Bract	MAC	2-Aminothiazole	Base activation	–	–	–	FT-IR, SEM, XPS	–	–	Lin *et al.* (2018)
Husk leaves	MAC	N,N-dimethylformamide and chloroacetyl chloride	–	100	–	720	FT-IR, XPS	–	–	Lin *et al.* (2019)
Stalk	MBC	–	–	500	–	–	Pore analyser, FT-IR, SEM, XRD	–	–	Liu *et al.* (2019)
Stalk	MBC	KOH	Base activation	–	–	–	Pore analyser, FT-IR, SEM, XRD	–	–	Liu *et al.* (2019)
Stalk	MBC	H_3PO_4	Acid activation	–	–	–	Pore analyser, FT-IR, SEM, XRD	–	–	Liu *et al.* (2019)
Cob	MAC	KOH	Base activation + pyrolysis	800	10	60	SEM, BET, Raman, FT-IR, XPS	1,054.20	–	Liu *et al.* (2020a)
Stalk	MAC	Citric acid	Acid activation	–	–	–	FT-IR, BET	45.30	–	Soldatkina & Yanar (2021)
Pericarp	MAC	KOH	Base activation + pyrolysis	627	6	93	BET, SEM, EDS	23.31	–	Loya-González *et al.* (2019)
Stalk	MBC	–	Pyrolysis	300	20	360	SEM, EDS, XPS, FT-IR	–	–	Ma *et al.* (2016)
Stalk	MAC	NaOH	Base activation	–	–	–	FT-IR, FE-SEM	–	–	Ma *et al.* (2017)
Straw	MAC	KOH	Base activation + Pyrolysis	800	5	60	FT-IR, EDS, XPS, BET	213.18	–	Ma *et al.* (2019)

(*Continued.*)

Table 1 | Continued

Plant parts	Adsorbent class	Modification/activation		Carbonization			Characterization	BET SSA (m^2/g)	Yield (wt %)	References
		Reagent/material	Process	Temp (°C)	Heating rate (°C/min)	Time (mins)				
Stalk	MB	–	–	–	–	–	–	–	–	Maghri *et al.* (2012)
Husk	MB	–	–	105	–	1,440	–	–	–	Malik *et al.* (2016)
Fibre	MAC	Isopropyl alcohol	–	–	–	–	EDS, SEM, FT-IR	–	–	Mallampati *et al.* (2015)
Cob	MAC	$CaCl_2$	Base activation	–	–	–	SEM, EDX	–	–	Manzoor *et al.* (2019)
Stigmata	MB	–	–	–	–	–	FT-IR, SEM	–	–	Mbarki *et al.* (2018)
Silk	MB	–	–	100	–	360	SEM, FT-IR	–	–	Miraboutalebi *et al.* (2017)
Cob	MAC	–	–	300	–	120	SEM, EDS, FT-IR	–	–	Miyah *et al.* (2016)
Cob	MBC	–	Pyrolysis	900	–	180	FT-IR, Raman, XRD, SEM	–	–	Mohanraj *et al.* (2020)
Stalk	MAC	–	Pyrolysis	500	–	240	SEM, FT-IR, BET	–	–	Mousavi *et al.* (2020)
Stalk	MAC	–	Pyrolysis	500	–	30	SEM, FT-IR	–	–	Mousavi *et al.* (2021)
Tassel	MAC	H_2SO_4	Acid activation	–	–	–	XRD, FT-IR	250.0	–	Moyo *et al.* (2013)
Cob	MB	–	–	–	–	–	–	–	–	Ibrahim (2013)
Stalk	MB	–	–	–	–	–	–	–	–	Muhammad *et al.* (2019)
Cob	MB	–	–	100	–	1,440	SEM, XRD, FT-IR	–	–	Muthusamy & Murugan (2016)
Silk	MC	–	–	–	–	–	SEM, XRD, FT-IR	–	–	Nadaroğlu *et al.* (2018)
Cob	MAC	–	Pyrolysis	500	20	120	SEM, TEM, XRD, VSM	–	–	Nethaji *et al.* (2013)
Cob	MAC	H_3PO_4	Acid activation	105	–	300	SEM, FT-IR	–	–	Ojediran *et al.* (2021)
Cob	MAC	H_3PO_4	Acid activation	105	–	300	FT-IR, SEM, EDX	–	–	Ojedokun & Bello (2017)
Cob	MAC	H_3PO_4 and $ZnCl_2$	Acid Pyrolysis + pyrolysis + salt activation	500	–	60	–	1,195.12	–	Okafor *et al.* (2015)

(*Continued.*)

Table 1 | Continued

Plant parts	Adsorbent class	Modification/activation		Carbonization			Characterization	BET SSA (m^2/g)	Yield (wt %)	References
		Reagent/material	Process	Temp (°C)	Heating rate (°C/min)	Time (mins)				
Tassel	MAC	–	Pyrolysis	500	–	60	FT-IR, SEM	–	–	Olorundare *et al.* (2014)
Cob	MC	–	–	–	–	–	FT-IR, SEM, EDX	–	–	Ong *et al.* (2017)
Husk	MB	–	–	–	–	–	FT-IR,	–	–	Paşka *et al.* (2014)
Husk	MC	–	–	–	–	–	FT-IR, XRD, SEM	–	–	Guin *et al.* (2018)
Stalk pith	MAC	Malic acid	Acid activation	–	–	–	SEM, EDS, XRD, FT-IR, XPS	–	–	Peng *et al.* (2021)
Silk	MB	–	–	–	–	–	SEM-EDX, ATR-FT-IR, BET	1.36	–	Petrović *et al.* (2016)
Silk	MB	–	–	–	–	–	SEM-EDX, ATR-FT-IR	1.36	–	Petrović *et al.* (2017)
Husk	MAC	NaOH	Base activation	–	–	–	SEM, ATR-FT-IR, BET, XRD	3.01	–	Ponce *et al.* (2021)
Cob	MAC	H_3PO_4	Acid activation	110	–	1,440	XRD, XPS, UV-DRS, PL, FT-IR, FE-SEM, BET, TEM	293.12	–	Ramamoorthy *et al.* (2020)
Cob	MAC	–	Pyrolysis	900	–	360	BET, TPD, TGA	–	–	Reddy *et al.* (2016)
Straw	MAC	$Zncl_2$	Salt activation	–	–	–	SEM, BET	937.0		Ren *et al.* (2020)
Pericarp	MB	–	–	–	–	–	SEM, ATR-FT-IR, BET	1.53	–	Rosas-Castor *et al.* (2014)
Cob	MB	–	–	–	–	–	FT-IR	–	–	Abubakar & Ibrahim (2018)
Cob	MB	–	–	–	–	–	FT-IR, BET, SEM	–	–	Pezhhanfar & Zarei (2021)
Husk	MB	–	–	–	–	–	FT-IR, BET, SEM	–	–	Pezhhanfar & Zarei (2021)
Cob	MB	–	–	120	–	1,440	–	–	–	Sallau *et al.* (2012)
Cob	MB	–	–	–	–	–	XRD, TDS, TSS	–	–	Saroj *et al.* (2015)
Cob leaves	MB	–	–	–	–	–	FT-IR	–	–	Sepúlveda *et al.* (2015)
Stalk	MAC	Cetylpyridinium bromide	Salt activation	–	–	–	FT-IR	42.6	–	Soldatkina & Zavrichko (2018)
Cob	MC	–	–	–	–	–	XRD, SEM, TEM, FT-IR, BET, VSM, XPS	23.10	–	Song *et al.* (2015)

(*Continued.*)

Table 1 | Continued

		Modification/activation		Carbonization						
Plant parts	Adsorbent class	Reagent/material	Process	Temp (°C)	Heating rate (°C/min)	Time (mins)	Characterization	BET SSA (m^2/g)	Yield (wt %)	References
Cob	MAC	Sulphuric acid	Acid activation	150	–	1,440	–	–	–	Ismail *et al.* (2018)
Stalk	MB	–	–	–	–	–	–	–	–	Taha *et al.* (2021)
Stalk	MAC	Sulphuric acid	Acid activation	–	–	–	–	–	–	Taha *et al.* (2021)
Stalk	MAC	Magnetic particles $FeSO_4.7H_2O$ and $FeCl_3.6H_2O$	–	–	–	–	–	–	–	Taha *et al.* (2021)
Cob	MAC	–	–	–	–	–	–	–	–	Tan *et al.* (2012)
Stalk	MAC	H_3PO_4	Acid activation	–	–	–	XPS, FT-IR	–	–	Tang *et al.* (2019)
Stalk	MAC	Maleic anhydride	Acid activation	–	–	–	XPS, FT-IR	–	–	Tang *et al.* (2021)
Cob	MB	–	–	–	–	–	FT-IR, SEM	–	–	Tejada-Tovar *et al.* (2021)
Cob	MBC	–	Pyrolysis	400	–	20	–	–	–	Tsamo *et al.* (2019)
Straw	MAC	Tetradecyltrimethyl ammonium bromide	Salt activation	–	–	–	FT-IR, BET, SEM	4.21	–	Umpuch & Jutarat (2013)
Cob	MAC	NaOH	Base activation	–	–	–	FT-IR	–	–	Velmurugan *et al.* (2016)
Stem tissue	MB	–	–	–	–	–	BET, FT-IR, SEM	7.23	–	Vučurović *et al.* (2014)
Cob	MAC	HCl	Acid activation + pyrolysis	700	–	60	FT-IR, SEM, BET	784.76	56.60	Wang *et al.* (2018)
Straw	MAC	$C_{17}H_{38}NBr$	Salt activation	–	–	–	–	–	–	Umpuch (2015)
Stalk	MAC	Triethylenetetramine	–	–	–	–	SEM, TEM	–	–	Wang *et al.* (2016)
Leaf	MBC	–	Pyrolysis	500	5.0	360	BET	2.72	–	Mu *et al.* (2020)
Tassel	MBC	–	Pyrolysis	500	5.0	360	BET	2.72	–	Mu *et al.* (2020)
Stalk	MBC	–	Pyrolysis	500	5.0	360	BET	2.72	–	Mu *et al.* (2020)
Root	MBC	–	Pyrolysis	500	5.0	360	BET	2.72	–	Mu *et al.* (2020)
Silk	MBC	–	Pyrolysis	500	5.0	360	BET	2.72	–	Mu *et al.* (2020)
Ear	MBC	–	pyrolysis	500	5.0	360	BET	2.72	–	Mu *et al.* (2020)
Cob	MBC	–	Pyrolysis	500	5.0	360	BET	2.72	–	Mu *et al.* (2020)
Stalk	MAC	Polyarcrylic acid	Acid activation	–	–	–	FE-SEM, FT-IR	–	–	Wen *et al.* (2018)
Cob	MAC	KOH		500	10.0	60		591.0	–	Wu *et al.* (2013)

(*Continued.*)

Table 1 | Continued

Plant parts	Adsorbent class	Modification/activation		Carbonization			Characterization	BET SSA (m^2/g)	Yield (wt %)	References
		Reagent/material	Process	Temp (°C)	Heating rate (°C/min)	Time (mins)				
			Pyrolysis and base activation				SEM, FT-IR, EDS, BET, thermal analyser			
Stalk	MAC	NaOH	Base activation	–	–	–	FT-IR, XRD, TG, SEM	–	–	Wu *et al.* (2017)
Cob	MB	–	–	–	–	–	FT-IR	–	–	Yaneva & Georgieva (2013)
Cob	MAC	H_3PO_4	Acid activation	–	–	–	FT-IR, BET	809.80	–	Zhang *et al.* (2014)
Stover	MAC	ZrO_2	–	–	–	–	BET	2.63	–	Zhang *et al.* (2016))
Cob	MBC	–	Pyrolysis	600	15	120	SEM, XRD, FT-IR, XPS, EPR	468.59	28.34	Zhang *et al.* (2020)
Straw	MAC	Glutamic acid	Acid activation	–	–	–	SEM, FT-IR	–	–	Zhao *et al.* (2014)
Cover	MC	–	–	–	–	–	XRD, EDX, SEM, FT-IR	–	–	Zolgharnein *et al.* (2016)

ATR (Attenuated total reflection), BET (Brunauer–Emmett–Teller), BJH (Barrett–Joyner–Halenda), UV-DRS (Ultraviolet–Visible Diffuse Reflectance Spectroscopy), EDS or EDX (Energy-dispersive X-ray spectroscopy), EDXRF (Energy Dispersive X-ray Fluorescence), EPR (Electron paramagnetic resonance), FT-IR-ATR (Fourier Transform Infrared Attenuated total reflection), PL (Photoluminescence emission spectra), PSO (Pseudo-second order), RE (Removal efficiency), SSA (specific surface area), SEM (Scanning Electron Microscopy, TDS (Total Dissolved Solids), TEM (Transmission electron microscopy), TG or TGA (Thermogravimetric analysis), TPD (Temperature programmed decomposition), TSS (Total Suspended Solids), VSM (vibrating sample magnetometer), XRD (X-ray Diffraction), XPS (X-ray photoelectron spectroscopy), XRF (X-ray photoelectron spectroscopy).

2.3. Maize activated carbon

MAC can be prepared by chemically activating UM or further activating the MBC analogue, as it has been established in a cow dung-based adsorbent review performed by Iwuozor *et al.* (2022b) that activation of biochar and its advanced treatment are essential for better adsorptive achievement. Empirically speaking, the MAC and MBC have parallel functional features except for a minor architectural disparity that is primarily linked to permeability. It is assumed that advanced activation of MBC enriches the biochar functional groups and also improves its porosity, which in turn affords extra binding sites for pollutant elimination as a result of increased surface area (Dehkhoda *et al.* 2016; Tan *et al.* 2017; Liu *et al.* 2018a; Li *et al.* 2019a). Holistically, according to literature, there are two distinct practices (physical and chemical) for producing MAC (Jun *et al.* 2010; Al-Swaidan & Ahmad 2011; Danish *et al.* 2011; Ekpete & Horsfall 2011; Yahya *et al.* 2015). In physical treatment, the matrix will first undergo carbonization and then be activated with steam or CO_2. Contrarily, in chemical treatment, the matrix is impregnated with an activating reagent and then carbonizes (pyrolytic decomposition of the biomass matrix) in a hypoxic atmosphere afterward (Solar *et al.* 2008; Yagmur *et al.* 2008; Giraldo & Moreno-Piraján 2012; Vicinisvarri *et al.* 2014). Notably, from several reports gathered in Table 1, during the preparation, most authors used a pre-carbonization activation tactic where the maize plant matrix was chemically activated using acid, base, or salt prior to actual carbonization. Meanwhile, the author provided no pragmatic explanation for the pre-carbonization activation practice selection. Nevertheless, it might be because pre-carbonization activation practice requires lower temperatures, gives a higher yield, produces a high surface area, requires a single step, creates fully grown micro-porousness, and reduces inorganic material composition, as expounded in some other reports (Budinova *et al.* 2006; Zhu *et al.* 2008; Hirunpraditkoon *et al.* 2011; Cruz *et al.* 2012; Yahya *et al.* 2015). Going forward, on a general note, the standard procedure before activation includes drying, pulverizing, and sieving to the desired particle size of the as-collected maize precursor. Furthermore, as shown in Table 1, most authors used H_3PO_4 for acid activation, KOH for base activation, and $ZnCl_2$ for salt activation. Basically, the role of the activating reagent is to function as a dehydrator and oxidant, avert the materialization of the ash or tar, and dissolve the cellulosic constituents of the matrix while introducing the interfacial organic oxygen moiety to the carbon of the matrix, stimulating the development of cross-links and carbon yield (Noor & Nawi 2008; Wang *et al.* 2010; Bello & Ahmad 2011; Campbell *et al.* 2012; Jassim *et al.* 2012; Mahapatra *et al.* 2012; Örkün *et al.* 2012; Yahya *et al.* 2015).

Ali *et al.* (2017), Zhang *et al.* (2014), and Aljeboree *et al.* (2019) used phosphoric acid as an activating agent, while Loya-González *et al.* (2019) and Liu *et al.* (2020a) used KOH as an activating agent. Briefly, during the chemical activation procedure, an amount of the activating reagent sufficient to create slurry was added to a weighed amount of the dried and size-reduced maize matrix. The slurry was agitated for a few seconds (usually $>$60 s) and then left to stand still for some time (usually a few hours). After that, the mixture's filtration residue is used to extract the activated maize matrix, which is then dried in an oven for some hours. To create the preferred MAC, the saturated and withered maize matrix was pyrolyzed in a furnace at various temperatures and times as reported in Table 1, followed by washing (usually with water) to obtain a benign sorbent product without impurity (Aljeboree *et al.* 2019; Loya-González *et al.* 2019; Campos *et al.* 2020). This MAC preparation methodology is consistent with the one adopted by Aljeboree & Alkaim (2019), Assirey & Altamimi (2021), Duru *et al.* (2019), Dutta & Nath (2018), and Peng *et al.* (2021) using H_2SO_4, HCl, tartaric acid, NaOH, and maleic acid, respectively.

2.4. Maize-based composite

Generally, the MC is functionalized collimate of MAC, MBC, or UM and is obtained through immobilization or impregnation of other materials such as graphene oxide (GO), nanoparticles such as TiO_2, Fe_3O_4, nZVI, etc., onto the UM, MAC, or MBC to enhance their adsorption performance by improving the mechanical strength, ease of separation after usage, and recyclability, among others. According to several authors (Panneerselvam *et al.* 2011; Gong *et al.* 2012; Heidari & Razmi 2012; Wang *et al.* 2014; Zolgharnein *et al.* 2016), the new resulting adsorbent comes with the increased potential for pollutant removal because this immobilization of other materials with some proper biosorbents gives a synergetic blend of advantages for both the biosorbents and the material. For example, GO can confer the new sorbent with an increasingly large number of oxygen-containing groups, while NPs can confer better photodegradation (Qu *et al.* 2020; Emmanuel & Adesibikan 2021; Emmanuel *et al.* 2023a) and excellent stability (Emmanuel *et al.* 2023b). The composite can be fabricated generally in two ways: first, by preparing the maize adsorbent and the Nanoparticles (NP)/GO separately before

blending them chemically, and second, by chemically blending the two materials at once. For instance, as reported by Qu *et al.* (2020), a corn cob biosorbent was first obtained by drying, pulverizing, sieving (60-mesh), and drying (at 60 °C) the virgin corn cob. Then GO was prepared as well by adding 1 g of graphene to 25 ml of concentrated H_2SO_4 for 60 sec, followed by the addition of 3.5 g of $KMnO_4$ in a container. Consequently, after 480 min of ultrasonic stripping, 46 ml of deionization was gradually added to the container to terminate the reaction. This was followed by the addition of 140 ml of distilled H_2O and 15 ml of 30% H_2O_2 to wash the product (GO) to neutrality, which was then dried at 60 °C. Subsequently, the GO/Corn Cob composites were fabricated by weighing 1.084 g of GO in 433.6 ml of deionized water. After the GO had fully dissolved, 17.344 g of corn cob biosorbent was slowly added and allowed to stand for 2 h, then later withered at 60 °C to achieve solid GO/Corn cob composites. This kind of two-step reaction approach was also used by Song *et al.* (2015) and Eltaweil *et al.* (2020) to prepare amine-functionalized magnetic corn stalk composites and nZVI/corn straw biochar composite, respectively. However, Zolgharnein *et al.* (2016) differ in their own approach by adopting a single-step reaction for the fabrication of a nano-Fe_3O_4/corn cover composite. Briefly, the right quantity of Fe_3O_4 NP and corn cover were ground thoroughly, followed by the addition of distilled water and thorough mixing in a shaker at 300 rpm for 48 h, and then dried in an oven at 70 °C for 5 h. It is imperative to mention here that the effect of the material ratio was not established nor explained, and this is very relevant like other preparation operating parameters. However, a number of researches have been carried out to boost the performance of MAC and MBC, such as the identification of the influence of pyrogenic temperature on adsorbent yield and surface morphology (Campbell *et al.* 2012; El-Sayed *et al.* 2014; Gao *et al.* 2019), the influence of various chemical activating agents on the output and architectural features of MAC (Dada *et al.* 2012), and the impact of various activators and impregnation proportions on MAC performance (Abdullah *et al.* 2019). Also, a number of characterization techniques have been employed to evaluate the architectural properties and morphological features of maize-based adsorbents, and they are summarized in Figure 2 based on the information they can supply.

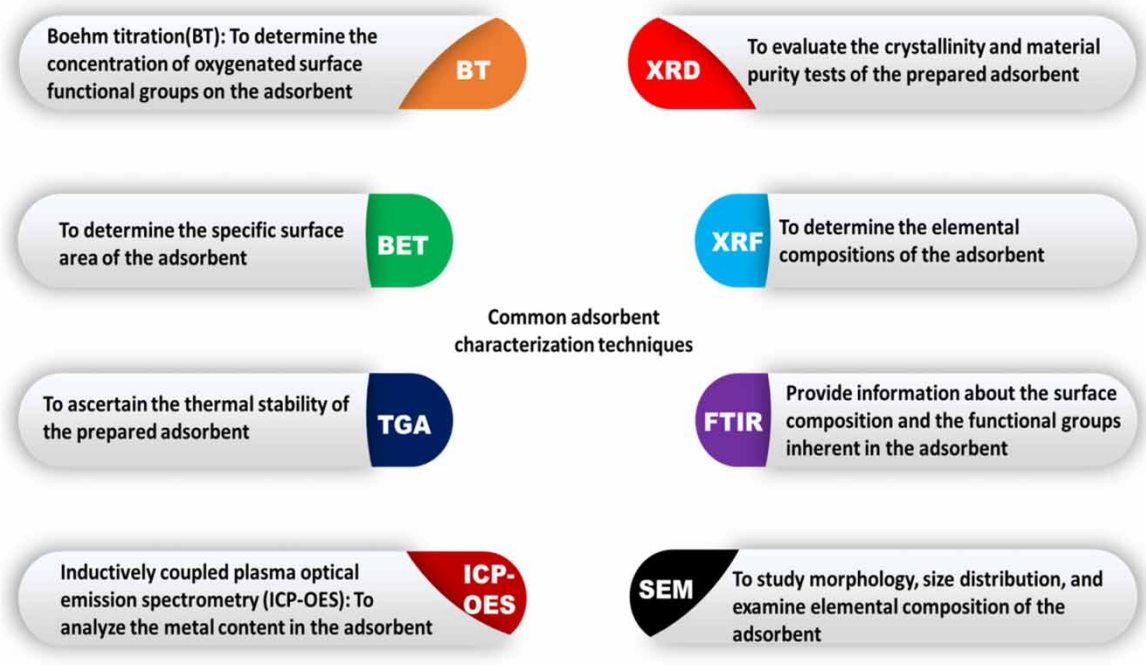

Figure 2 | Common instrumental methods of analysis for studying the morphological and architectural properties of maize-based adsorbents.

3. ADSORBENT PERFORMANCE OF MAIZE/CORN-BASED ADSORBENTS

An adsorbent's adsorptive ability is a crucial determinant of its application assessment. In Table 2, the ability of various corn-based adsorbents to remove contaminants from aqueous solutions is shown. The effectiveness of an adsorbent in removing a given pollutant is typically determined by two factors: adsorption capacity and removal

Table 2 | Adsorption performance of maize/corn adsorbents for dye uptake

Plant parts	Adsorbent class	Adsorbate dye	RE%	q_{max} (mg/g)	Dosage (g/L)	pH	Temp (°C)	SSA (m^2/g)	Method of q_{max} determination	References
Cob	MAC	Gentian violet	–	700.0	–	3.0	–	–	Dubinin-Radushkevich	Javed *et al.* (2021)
Cob	MAC	Methyl orange	–	555.56	–	6.5	25	784.76	Langmuir	Wang *et al.* (2018)
Cob	MAC	Malachite green	94.48	313.63	1.0	12.0	25	–	Langmuir	Farnane *et al.* (2018)
Cob	MAC	Methylene blue	99.98	271.19	1.0	12.0	25	–	Langmuir	Farnane *et al.* (2018)
Cob	MAC	Methylene blue	–	216.60	0.1	5.6	30	–	Langmuir	Jawad *et al.* (2018)
Cob	MAC	Indigo carmine	90.13	118.48	–	–	25	809.80	Langmuir	Zhang *et al.* (2014)
Cob	MAC	Methylene blue	–	100.0	0.02	7.0	–	650.0	Langmuir	Reddy *et al.* (2016)
Cob	MAC	Congo red	–	98.72	1.0	7.0	35	–	Langmuir	Velmurugan *et al.* (2016)
Cob	MAC	Maxilone	–	86.89	0.1	10.0	45	–	Langmuir	Aljeboree & Alkaim (2019)
Cob	MBC	Methyl orange	–	86.38	–	–	–	468.59	Langmuir	Zhang *et al.* (2020)
Cob	MB	Malachite green	92.11	76.42	4.0	12.0	25	–	Langmuir	Farnane *et al.* (2018)
Cob	MB	Methylene blue	94.41	75.27	4.0	12.0	25	–	Langmuir	Farnane *et al.* (2018)
Cob	MAC	Tartrazine	76.90	68.78	–	–	25	809.80	Langmuir	Zhang *et al.* (2014)
Cob	MAC	Malachite green	99.3	66.52	–	6.0	–	13.29	Langmuir	Ojediran *et al.* (2021)
Cob	MAC	Congo red	–	50.0	–	–	30	–	Langmuir	Ojedokun & Bello (2017)
Cob	MAC	Methylene blue	96.0	46.28	2.0	12.0	20	–	Experiments	Miyah *et al.* (2016)
Cob	MAC	Methylene blue	–	41.94	0.1	10.0	45	–	Langmuir	Aljeboree & Alkaim (2019)
Cob	MAC	Methylene blue	–	37.45	0.5	6.0	50	–	Langmuir	Aljeboree *et al.* (2019)
Cob	MC	Malachite green	–	35.34	–	4.0	–	–	Langmuir	Ong *et al.* (2017)
Cob	MAC	Crystal violet	–	33.86	0.1	10.0	45	–	Langmuir	Aljeboree & Alkaim (2019)
Cob	MAC	Methylene blue	99.40	28.65	2.0	8.0	25	700.00	Langmuir	El-Sayed *et al.* (2014)
Cob	MAC	Sulfur dioxide	–	19.8	–	–	–	591.0	Experiments	Wu *et al.* (2013)
Cob	MAC	Methylene blue	44.60	17.75	2.0	8.0	25	633.00	Langmuir	El-Sayed *et al.* (2014)
Cob	MB	Methylene blue	–	16.08	–	6.5	–	0.40	Langmuir	Pezhhanfar & Zarei (2021)
Cob	MB	Congo red	–	4.83	–	7.0	–	–	Experiments	Yaneva & Georgieva (2013)
Cob	MAC	Methylene blue	92.20	0.81	2.0	8.0	25	600.00	Langmuir	El-Sayed *et al.* (2014)
Cob	MC	Acid yellow	–	0.24	–	4.0	–	–	Langmuir	Ong *et al.* (2017)
Cob	MAC	Methylene blue	99.90	–	5.0	–	–	–	Experiments	Ali *et al.* (2017)

(*Continued.*)

Table 2 | Continued

Plant parts	Adsorbent class	Adsorbate dye	RE%	q_{max} (mg/g)	Dosage (g/L)	pH	Temp (°C)	SSA (m^2/g)	Method of q_{max} determination	References
Cob	MAC	Methylene blue	99.89	–	10.0	6.0	27	–	Experiments	Tan *et al.* (2012)
Cob	MAC	Brilliant green	99.60	–	5.0	–	–	–	Experiments	Ali *et al.* (2017)
Cob	MAC	Malachite green	99.39	–	10.0	7.0	29	–	Experiments	Ismail *et al.* (2018)
Cob	MAC	Congo red	98.10	–	0.3	6.8	27	–	Experiments	Leelavathy *et al.* (2015)
Cob	MAC	Congo red	97.80	–	1.2	6.8	27	–	Experiments	Leelavathy *et al.* (2015)
Cob	MB	Methylene blue	96.94	–	0.4	5.0	–	–	Langmuir	Fatoye & Onigbinde (2020)
Cob	MB	Bromophenol blue	96.53	–	4.0	2.0	–	–	Experiments	Abubakar & Ibrahim (2018)
Cob	MB	Bromothymol blue	94.39	–	0.5	2.0	–	–	Experiments	Abubakar & Ibrahim (2018)
Cob	MC	Congo red	91.28	–	1.2	3.0	30	–	Experiments	Qu *et al.* (2020)
Cob	MAC	Methylene blue	90.86	–	0.2	7.0	–	293.12	Experiments	Ramamoorthy *et al.* (2020)
Cob	MB	Direct blue 199	90.0	–	8.0	7.6	28	–	Experiments	Saroj *et al.* (2015)
Cob	MBC	Methylene blue	82.0	–	–	–	–	–	Experiments	Mohanraj *et al.* (2020)
Cob	MAC	Methyl orange	80.36	–	5.0	–	25	–	Experiments	Abdullah *et al.* (2019)
Cob	MB	Congo red	80.21	–	1.2	3.0	30	–	Experiments	Qu *et al.* (2020)
Cob	MBC	Rhodamine B	80.0	–	–	–	–	–	Experiments	Mohanraj *et al.* (2020)
Cob	MBC	Methylene blue	64.0	–	–	8.0	25	–	Experiments	Tsamo *et al.* (2019)
Cob	MBC	Methylene blue	33.38	–	–	–	25	2.72	Experiments	Mu *et al.* (2020)
Cob leaves	MB	Basic violet 4	98.4	89.0	2.0	5.4	57	–	Langmuir	Sepúlveda *et al.* (2015)
Cover	MC	Alizarin red S	–	10.5	0.2	2.0	–	–	Langmuir	Zolgharnein *et al.* (2016)
Ear	MBC	Methylene blue	44.13	–	–	–	25	2.72	Experiments	Mu *et al.* (2020)
Fibre	MAC	Alcian blue		159.0	–	7.0	–	–	Experiments	Mallampati *et al.* (2015)
Fibre	MAC	Methylene blue	–	70.0	–	7.0	–	–	Experiments	Mallampati *et al.* (2015)
Fibre	MAC	Neutral red	–	50.0	–	7.0	–	–	Experiments	Mallampati *et al.* (2015)
Fibre	MAC	Coomaise brilliant blue	–	35.0	–	7.0	–	–	Experiments	Mallampati *et al.* (2015)
Husk	MC	Methylene blue	–	1,682.7	–	9.0	47	–	Langmuir	Guin *et al.* (2018)
Husk	MAC	Methylene blue	–	662.25	0.3	4.0	45	–	Langmuir	Khodaie *et al.* (2013)
Husk	MB	Methylene blue	–	50.69	2.0	6.0	25	–	Langmuir	Paşka *et al.* (2014)
Husk	MB	Methylene blue	90.0	30.30	–	6.2	28	–	Langmuir	Malik *et al.* (2016)

(*Continued.*)

Table 2 | Continued

Plant parts	Adsorbent class	Adsorbate dye	RE%	q_{max} (mg/g)	Dosage (g/L)	pH	Temp (°C)	SSA (m^2/g)	Method of q_{max} determination	References
Husk	MB	Methylene blue	–	20.66	–	6.5	–	2.49	Langmuir	Pezhhanfar & Zarei (2021)
Husk	MAC	Methylene blue	98.50	–	5.0	10.3	25	3.01	Experiments	Ponce *et al.* (2021)
Husk leaf	MAC	Malachite green	–	81.50	2.5	6.0	50	–	Langmuir	Jalil *et al.* (2012)
Leaf	MBC	Methylene blue	89.32	–	–	–	25	2.72	Experiments	Mu *et al.* (2020)
Leaves	MAC	Methyl orange	93.00	13.85	–	9.0	30	–	Langmuir	Fadhil & Eisa (2019)
Leaves	MAC	Methyl orange	71.00	4.93	–	9.0	30	–	Langmuir	Fadhil & Eisa (2019)
Leaves	MAC	Malachite green	91.5	–	2.5	5.8	3.0	–	Langmuir	Fadhel *et al.* (2021)
Leaves	MAC	Indigo carmen	91.0	–	0.3	12.0	30	–	Langmuir	Fadhil *et al.* (2021)
Pericarp	MAC	Methyl orange	50.0	141.13	–	–	–	23.31	Experiments	Loya-González *et al.* (2019)
Pericarp	MB	Methylene blue	–	110.90	1.0	8.0	35	1.53	Langmuir	Rosas-Castor *et al.* (2014)
Pith	MAC	Malachite green	–	488.3	1.6	7.0	30	0.01	Langmuir	Jothirani *et al.* (2016)
Porous starch	MAC	Neutral red	–	13.05	–	–	–	196.88	Experiments	Guo *et al.* (2015b)
Porous starch	MAC	Methylene blue	–	12.94	–	–	–	196.88	Experiments	Guo *et al.* (2015b)
Root	MBC	Methylene blue	41.12	–	–	–	25	2.72	Experiments	Mu *et al.* (2020)
Silk	MB	Methylene blue	–	234.10	–	12.0	–	–	Langmuir	Miraboutalebi *et al.* (2017)
Silk	MB	Reactive blue 19	99.00	71.60	5.0	2.0	25	–	Langmuir	Değermenci *et al.* (2019)
Silk	MB	Reactive red 218	99.00	63.30	5.0	2.0	25	–	Langmuir	Değermenci *et al.* (2019)
Silk	MC	Direct blue 15	99.76	–	–	3.0	25	–	Experiments	Nadaroğlu *et al.* (2018)
Silk	MBC	Methylene blue	20.94	–	–	–	25	2.72	Experiments	Mu *et al.* (2020)
Stalk	MAC	Methylene blue	94.0	870.0	0.1	7.0	–	–	Langmuir	Tang *et al.* (2021)
Stalk	MAC	Congo red	–	549.0	–	–	–	201.0	Experiments	Li *et al.* (2019b)
Stalk	MB	Methylene blue	–	500.0	4.0	6.8	–	–	Langmuir	Maghri *et al.* (2012)
Stalk	MBC	Methylene blue	100.0	406.43	–	11.0	–	–	Langmuir	Liu *et al.* (2019)
Stalk	MAC	Methylene blue	–	370.0	–	11.0	–	–	Langmuir	Wen *et al.* (2018)
Stalk	MAC	Coomaise brilliant blue	–	302.0	–	–	–	201.0	Experiments	Li *et al.* (2019)b
Stalk	MBC	Methylene blue	86.0	230.39	–	11.0	–	–	Langmuir	Liu *et al.* (2019)
Stalk	MAC	Methylene blue	97.0	129.0	2.0	9.0	35	–	Langmuir	Tang *et al.* (2019)
Stalk	MB	Crystal violet	82.0	120	0.1	10.0	–	–	Experiments	Muhammad *et al.* (2019)

(*Continued.*)

Table 2 | Continued

Plant parts	Adsorbent class	Adsorbate dye	RE%	q_{max} (mg/g)	Dosage (g/L)	pH	Temp (°C)	SSA (m^2/g)	Method of q_{max} determination	References
Stalk	MAC	Methylene blue	99.70	49.01	0.2	–	50	–	Experiments	Ma *et al.* (2017)
Stalk	MBC	Methylene blue	41.0	43.14	–	11.0	–	–	Langmuir	Liu *et al.* (2019)
Stalk	MAC	Acid orange	–	31.06	–	3.0	30	42.60	Langmuir	Soldatkina & Zavrichko (2018)
Stalk	MAC	Acid red	–	30.77	–	3.0	30	42.60	Langmuir	Soldatkina & Zavrichko (2018)
Stalk	MAC	Malachite green	–	27.55	–	6.0	60	45.3	Langmuir	Soldatkina & Yanar (2021)
Stalk	MAC	Direct red 23	99.00	27.11	0.2	3.0	25	–	Langmuir	Fathi *et al.* (2015)
Stalk	MAC	Methylene blue	–	26.60	–	6.0	60	45.3	Langmuir	Soldatkina & Yanar (2021)
Stalk	MB	Malachite green	–	11.77	–	6.0	–	4.79	Langmuir	Lara-Vásquez *et al.* (2016)
Stalk	MAC	Methylene blue	–	8.75	–	–	–	–	Langmuir	Wu *et al.* (2017)
Stalk	MAC	Rhodamine B	89.60	5.60	2.5	3.0	–	–	Langmuir	Mousavi *et al.* (2021)
Stalk	MAC	Methylene blue	99.50	2.34	1.4	11.0	–	–	Langmuir	Mousavi *et al.* (2020)
Stalk	MBC	Phenol	95.88	–	–	–	25	325.90	Experiments	Li *et al.* (2019a)
Stalk	MB	Malachite green	90.00	–	–	7.0	–	–	Experiments	Abubakar & Batagarawa (2017)
Stalk	UM	Coomaise brilliant blue	85.0	–	2.0	3.0	25	–	Experiments	Taha *et al.* (2021)
Stalk	MB	Congo red	84.70	–	–	–	–	–	Experiments	Abubakar & Batagarawa (2017)
Stalk	MAC	Coomaise brilliant blue	80.0	–	2.0	3.0	25	–	Experiments	Taha *et al.* (2021)
Stalk	MAC	Alizarin yellow	75.85	–	0.6	–	30	–	Langmuir	Ismail *et al.* (2019)
Stalk	MAC	Coomaise brilliant blue	50.0	–	4.0	3.0	25	–	Experiments	Taha *et al.* (2021)
Stalk	MBC	Methylene blue	23.32	–	–	–	25	2.72	Experiments	Mu *et al.* (2020)
Stalk + walnut shell	MAC	Malachite green	–	450.78	–	–	20	1,187.00	Langmuir	Kang *et al.* (2018)
Stalk pith	MAC	Crystal violet	–	566.27	0.25	10	45	–	Experiments	Peng *et al.* (2021)
Stalk pith	MAC	Methylene blue	–	422.13	0.25	10	25	–	Experiments	Peng *et al.* (2021)
Starch	MAC	Tartrazine	–	293.0	–	2.5	35	–	Langmuir	Dai *et al.* (2017)
Starch	MB	Methylene blue	–	6.40	–	–	–	0.42	Experiments	Guo *et al.* (2015b)
Starch	MB	Neutral red	–	5.87	–	–	–	0.42	Experiments	Guo *et al.* (2015b)

(*Continued.*)

Table 2 | Continued

Plant parts	Adsorbent class	Adsorbate dye	RE%	q_{max} (mg/g)	Dosage (g/L)	pH	Temp (°C)	SSA (m^2/g)	Method of q_{max} determination	References
Stem	MAC	Bromophenol blue	–	–	–	–	–	–	Experiments	Dada *et al.* (2012)
Stem	MAC	Methyl orange solution	–	–	–	–	–	–	Experiments	Dada *et al.* (2012)
Stem tissue	MB	Eriochrome black T	66.80	167.01	1.0	2.0	25	7.23	Langmuir	Vučurović *et al.* (2014)
Stem tissue	MB	Methylene blue	99.90	160.84	1.0	6.0	25	7.23	Langmuir	Vučurović *et al.* (2014)
Stigmata	MB	Methylene blue	33.90	106.30	–	7.0	–	–	Experiments	Mbarki *et al.* (2018)
Stigmata	MB	Indigo carmine	69.68	63.70	–	2.0	–	–	Experiments	Mbarki *et al.* (2018)
Stover	MAC	Reactive red 141	–	15.65	3.0	3.0	–	0.69	Langmuir	Carijo *et al.* (2019)
Straw	MAC	Rhodamine B	–	1,578.0	–	7.0	–	1,993.00	Langmuir	Chen *et al.* (2019)
Straw	MB	Malachite green	–	524.25	–	6.0	55	0.85	Experiments	Lima *et al.* (2018)
Straw	MBC	Malachite green	99.00	515.77	0.3	6.0	25	80.10	Langmuir	Eltaweil *et al.* (2020)
Straw	MB	Malachite green	77.0	200.0	0.5	6.0	55	0.85	Experiments	Lima *et al.* (2017)
Straw	MAC	Methylene blue	–	196.46	–	6.0	60	–	Experiments	Zhao *et al.* (2014)
Straw	MAC	Reactive brilliant red K-2BP	83.40	178.75	2.0	3.0	45	937.0	Langmuir	Ren *et al.* (2020)
Straw	MAC	Green 40	–	152.75	–	2.0	–	–	Langmuir	Umpuch (2015)
Straw	MAC	Reactive brilliant yellow K-6G	79.30	140.84	2.0	3.0	45	937.0	Langmuir	Ren *et al.* (2020)
Straw	MAC	Yellow 20	95.67	–	–	2.0	–	4.21	Experiments	Umpuch & Jutarat (2013)
Straw	MAC	Blue 21	94.70	–	–	2.0	–	4.21	Experiments	Umpuch & Jutarat (2013)
Straw + waste red mud	MBC	Acidic black	–	70.90	–	1.0	–	20.34	Experiments	Gao *et al.* (2021)
Straw pith	MAC	Malachite green	–	242.13	–	12.0	25	–	Langmuir	Chen *et al.* (2020)
Straw pith	MAC	Methylene blue	–	215.05	–	12.0	25	–	Langmuir	Chen *et al.* (2020)
Straw pith	MAC	Rhodamine B	–	213.68	–	12.0	25	–	Langmuir	Chen *et al.* (2020)
Tassel	MAC	Methylene blue	–	200.0	–	10.0	30	–	Langmuir	Olorundare *et al.* (2014)
Tassel	MBC	Methylene blue	59.08	–	–	–	25	2.72	Experiments	Mu *et al.* (2020)
Tassel powder	MAC	Reactive red 198	97.00	16.95	2.0	3.0	–	–	Langmuir	Dehvari *et al.* (2013)

efficiency. While pollutant removal efficiency depends on the pollutant concentration, adsorbent dosage, and competing ions in the system, adsorption capacity is an inherent property of an adsorbent towards the pollutant (Emenike *et al.* 2021, 2022a). The adsorption capacity is ascertained either experimentally or using isothermal parameters (Emenike *et al.* 2022b). As illustrated in Table 2, additional variables that influence an adsorbent's ability include the solution pH, temperature, and amount of the adsorbent. The surface area, which reveals the porosity and degree of active sites on the adsorbent, is another important contributing component.

Corn husks have been studied by Ponce *et al.* (2021) for their potential to remove methylene blue from liquids. The polymeric component of the fibre was removed from the biowaste using a 0.10 mol/L NaOH solution, which also helped to increase dye's adsorption. Characterization revealed that the main components of the corn husk adsorbent, which has a BET surface area of 3.01 m^2/g, are cellulose, hemicellulose, and lignin. More than 90% of the dye was removed in 2 h, according to the adsorption analysis, which demonstrated that the alkali treatment boosted adsorbent's attractiveness towards the adsorbate. A composite made of corncob and GO was created by Qu *et al.* (2020), and its efficacy in the adsorptive removal of Congo red from wastewater was investigated. The outcome demonstrated the presence of many functional groups in the composite, including hydroxyl, carboxyl, phenol, and alcohol groups, which provided enough binding sites and facilitated dye adsorption. The amount of dye removed rose in response to an increase in adsorbent dosage and reached 80% in 60 min. The process was endothermic and involved chemical adsorption mechanisms. Similar to this, Zolgharnein *et al.* (2016) evaluated the efficacy of a composite sorbent for the removal of Alizarin red S dye from liquids by impregnating Fe_3O_4 nanoparticles onto corn cover in a ratio of 1:10. At ideal pH of 2, an adsorbent dosage of 0.2 g, and dye concentration of 10 mg/L, a maximum adsorption capacity of 11.35 mg/g, and a removal efficiency of 80.1% were achieved. The adsorption results were well fitted by pseudo-second-order kinetic, Langmuir, Freudlich, and Dubinin–Radushkevich isotherm models, whereas thermodynamic investigations suggested a spontaneous and exothermic process.

Li *et al.* (2019b) synthesized a cellulose-rich aerogel in a single step by using a linked solvent system to separate lignin from other corn stalk constituents. The aerogel has a huge surface area (201 m^2/g), a porous, three-dimensional structure, and good thermal stability. Congo red and Coomassie brilliant blue had maximum adsorption capacities of 549 and 302 mg/g, respectively, according to a simulation of the aerogel adsorbent in dye-contaminated water. The study offers a practical, eco-friendly method for producing corn stalk material with good water treatment capabilities. Furthermore, Eltaweil *et al.* (2020) investigated the potential of a composite prepared from corn stalk biochar (CSB) and zero-valent iron nanoparticles (nZVI) to adsorb malachite green dye from solution. The results of the various techniques used to analyse the composite adsorbent, including FT-IR, XRD, SEM, and TGA, showed that it was a magnetic composite with a mesoporous structure, several functional groups, and a large surface area (80.1 m^2/g). The adsorption data involved both adsorption and oxidation mechanisms, with a removal efficiency of up to 99.9% attained in 20 min. They also fit well with second-order reaction kinetics and the Langmuir isotherm. Comparing the adsorbent to the individual components (CSB and nZVI), it also demonstrated a higher adsorption capacity (515.77 mg/g), and its magnetic property makes separation easier. The summary of the findings is presented in Table 2.

4. MECHANISM OF DYE ADSORPTION BY MAIZE-BASED ADSORBENTS

In the chemistry of adsorption for pollution remediation, the key difficulty is choosing the most auspicious adsorbent materials, particularly those with the best combination of low cost, remarkable adsorption potential, excellent adsorption efficiency, good selectivity, and swift kinetics. To overcome these challenges, a grounded understanding of the adsorption mechanism is required. Besides, understanding the adsorption mechanism will offer a win–win insight into designing outstanding desorption tactics for the reclamation of decontaminated contaminants and the recyclability of spent adsorbents (Crini 2005; Crini *et al.* 2019). However, in a bid to undoubtedly pinpoint the adsorption mechanism(s) (particularly the adsorbent–adsorbate interface interactions) so as to easily overcome those aforementioned challenges and take the adsorption process to the next level, this also becomes another real challenge and is now an important topic (Crini 2005; Crini *et al.* 2019). Practically speaking, according to Crini *et al.* (2019), adsorption is simply a shift in an adsorbate molecule's concentration in the outer layer of a solid adsorbent matrix compared with the core layer per unit surface area. This simple explanation about adsorption is consistent with that of Sanghi & Verma (2013), who also accentuated that in the adsorption phenomenon, the accumulation or concentration of a substance (adsorbate) takes place at the

adsorbent surface or interface compared with the bulk phase. However, to be perfectly frank, amid all these clear, real, simple, and practicable explanations of adsorption, its mechanistic operation is not wholly understood yet owing to the fact that there are so many potential interactions as shown in Figure 3, and the adsorbate properties (dissolution rate or miscibility, pKa, etc.), the analytical parameters (ionic strength, temperatures, kinetics), and the features of the adsorbent (surface area and architectural functional groups) all have a significant impact on these interactions (Crini 2005; Crini *et al.* 2019; Iwuozor *et al.* 2022b). But still, according to Crini *et al.* (2019), there is an intriguing query: Do the aforementioned interactions have to be considered to fully comprehend the adsorption mechanism? Well, this question's response is somewhat complicated. Depending on the adsorbent architectural makeup, the pollutant makeup and its characteristics, the solution pH, and the ionic strength, it is feasible that more than one of these interactions can take place concurrently in an adsorption process, as shown in the reports of previous studies (Yaneva & Georgieva 2013; Song *et al.* 2015; Guo *et al.* 2018; Soldatkina & Zavrichko 2018; Liu *et al.* 2019; Li *et al.* 2019a, 2019b; Zhang *et al.* 2020; Pezhhanfar & Zarei 2022) (Table 3).

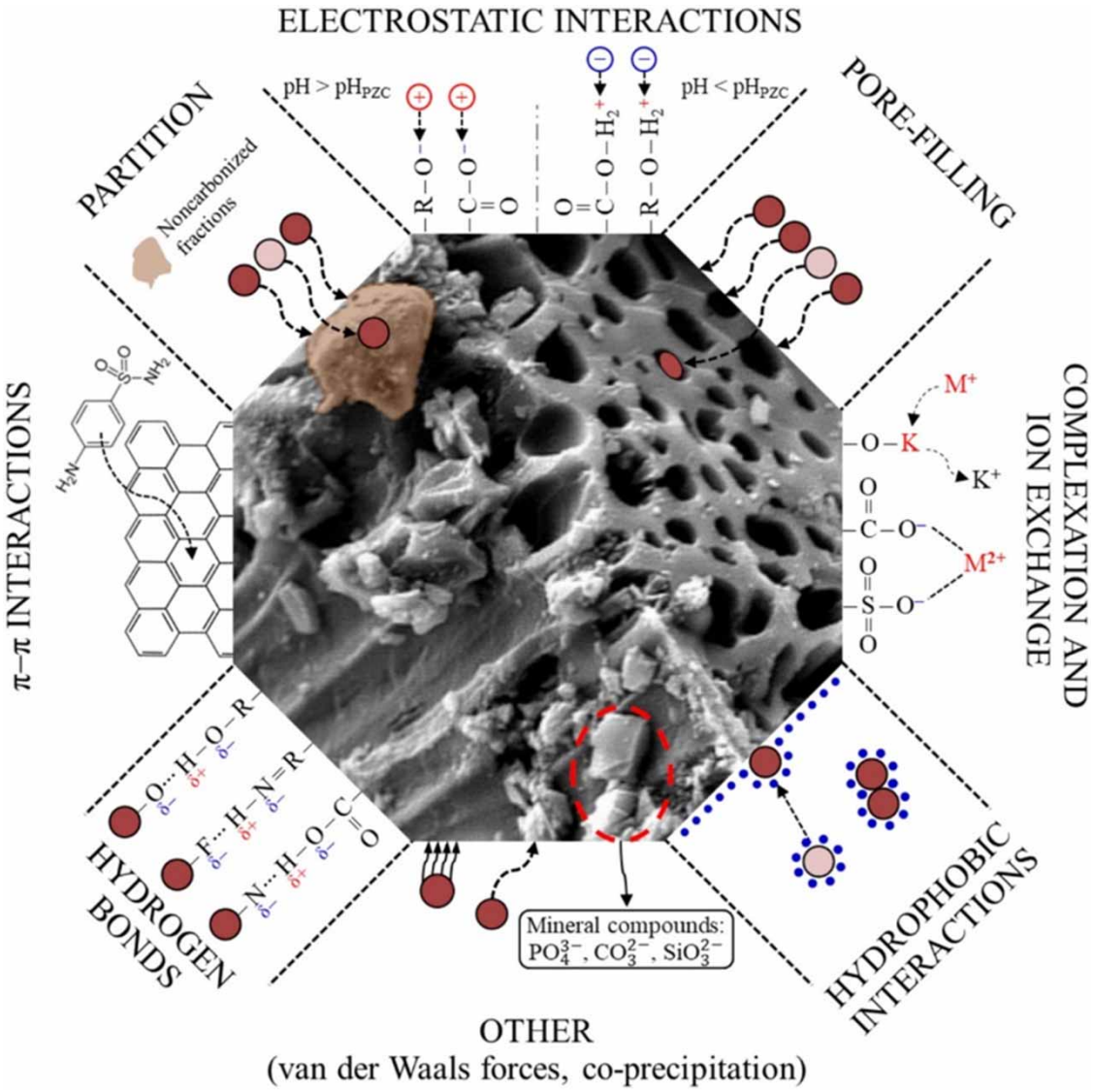

Figure 3 | Plausible mechanistic corn adsorbent–adsorbate interactions (Barquilha & Braga 2021).

Furthermore, it is interesting to say that since the adsorption phenomenon is invariably influenced by the aforementioned experimental conditions, isotherm and kinetics models of best-fit hypotheses as well as thermodynamic parameters can be used in some cases to open up adsorbent–adsorbate interaction mysteries and identify the most plausible adsorption mechanism (Abdelwahab 2008; Danish *et al.* 2011; Iwuozor *et al.* 2022b). For instance, Guo *et al.* (2018) established in their study that the adsorption mechanism of tylosin

Table 3 | Optimum pH and mechanism for dye uptake by maize/corn adsorbents

Plant parts	Adsorbent class	Dye	Optimum pH	pHzc	Adsorption mechanism	References
Cob	MB	Methylene blue	6.5	–	$\pi-\pi$ interaction, hydrogen bonds	Pezhhanfar & Zarei (2021)
Husk	MB	Methylene blue	6.5	–	$\pi-\pi$ interaction, hydrogen bonds	Pezhhanfar & Zarei (2021)
Stalk	MBC	Phenol	–	–	Pore-filling, electrostatic attraction, $\pi-\pi$ interaction	Li *et al.* (2019)a
Stalk	MAC	Acid red	3.0	5.1	Ion exchange, chemisorption	Soldatkina & Zavrichko (2018)
Stalk	MAC	Acid orange	3.0	5.1	Ion exchange, chemisorption	Soldatkina & Zavrichko (2018)
Stalk	MAC	Congo red	–	–	Hydrogen bonding, $\pi-\pi$ interaction	Li *et al.* (2019b)
Stalk	MAC	Coomaise brilliant blue	–	–	Hydrogen bonding, $\pi-\pi$ interaction	Li *et al.* (2019b)
Pericarp	MB	Methylene blue	8.0	3.6	Electrostatic repulsion	Rosas-Castor *et al.* (2014)
Cob	MB	Congo red	7.0	7.2	Electrostatic interactions, H-bonding, hydrophobic–hydrophobic interactions	Yaneva & Georgieva (2013)
Cob	MBC	Methyl orange	–	–	Electrostatic interactions, electron sharing, electron exchange	Zhang *et al.* (2020)
Silk	MB	Reactive blue 19	12.0	–	Electrostatic interactions	Değermenci *et al.* (2019)
Silk	MB	Reactive red 218	12.0	–	Electrostatic interactions	Değermenci *et al.* (2019)
Stalk	MAC	Methylene blue	11.0	–	Electrostatic interactions	Wen *et al.* (2018)
Stem tissue	MB	Methylene blue	6.0	2.4	Electrostatic interactions	Vučurović *et al.* (2014)
Stem tissue	MB	Eriochrome black T	2.0	2.4	Electrostatic interactions	Vučurović *et al.* (2014)
Straw	MAC	Green 40	2.0	–	Electrostatic interactions	Umpuch (2015)
Stalk	MBC	Methylene blue	11.0	–	Electrostatic interaction, hydrogen bonding, $\pi-\pi$ stacking, physical interaction	Liu *et al.* (2019)
Straw	MAC	Tylosin	12.0	–	Electrostatic interaction, H-bonding and hydrophobic interactions	Guo *et al.* (2018)
Straw	MAC	Tylosin	12.0	–	Electrostatic interaction, H-bonding and hydrophobic interactions	Guo *et al.* (2018)
Straw	MB	Tylosin	12.0	–	Electrostatic interaction, H-bonding and hydrophobic interactions	Guo *et al.* (2018)
Stalk	MAC	Direct red 23	12.0	–	Electrostatic interaction, chemical reaction	Fathi *et al.* (2015)
Cob	MB	Congo red	3.0	–	Electrostatic interaction	Qu *et al.* (2020)
Cob	MC	Congo red	3.0	–	Electrostatic interaction	Qu *et al.* (2020)
Cob leaves	MB	Basic violet 4	5.4	4.1	Electrostatic interaction	Sepúlveda *et al.* (2015)
Pith	MAC	Malachite green	7.0	–	Electrostatic interaction	Jothirani *et al.* (2016)

(*Continued.*)

Table 3 | Continued

Plant parts	Adsorbent class	Dye	Optimum pH	pHzc	Adsorption mechanism	References
Stalk	MAC	Rhodamine B	3.0	–	Electrostatic interaction	Mousavi *et al.* (2021)
Stigmata	MB	Methylene blue	7.0	–	Electrostatic interaction	Mbarki *et al.* (2018)
Cob	MAC	Gentian violet	3.0	3.15	Electrostatic attraction	Javed *et al.* (2021)
Cob	MAC	Congo red	7.0	–	Electrostatic attraction	Velmurugan *et al.* (2016)
Cob	MB	Bromophenol blue	2.0	5.0	Electrostatic attraction	Abubakar & Ibrahim (2018)
Cob	MB	Bromothymol blue	2.0	5.0	Electrostatic attraction	Abubakar & Ibrahim (2018)
Husk	MB	Methylene blue	6.2	–	Electrostatic attraction	Malik *et al.* (2016)
Stalk	MAC	Methylene blue	11.0	5.0	Electrostatic attraction	Mousavi *et al.* (2020)
Stalk	MAC	Methylene blue	9.0	5.7	Electrostatic attraction	Tang *et al.* (2019)
Stalk	MAC	Methylene blue	7.0	4.8	Electrostatic attraction	Tang *et al.* (2021)
Stigmata	MB	Indigo carmine	2.0	–	Electrostatic attraction	Mbarki *et al.* (2018)
Straw	MAC	Reactive brilliant yellow K-6G	3.0	–	Electrostatic attraction	Ren *et al.* (2020)
Straw	MAC	Reactive brilliant red K-2BP	3.0	–	Electrostatic attraction	Ren *et al.* (2020)
Straw	MAC	Methylene blue	6.0	–	Electrostatic attraction	Zhao *et al.* (2014)
Tassel	MAC	Methylene blue	10.0	–	Electrostatic attraction	Olorundare *et al.* (2014)
Stalk	MB	Crystal violet	10.0	–	Chemisorption	Muhammad *et al.* (2019)
Cob	MAC	Methylene blue	11.0	–	–	Ali *et al.* (2017)
Cob	MAC	Brilliant green	11.0	–	–	Ali *et al.* (2017)
Cob	MAC	Methylene blue	10.0	–	–	Aljeboree & Alkaim (2019)
Cob	MAC	Crystal violet	10.0	–	–	Aljeboree & Alkaim (2019)
Cob	MAC	Maxilone	10.0	–	–	Aljeboree & Alkaim (2019)
Cob	MAC	Methylene blue	6.0	–	–	Aljeboree *et al.* (2019)
Cob	MAC	Acetic acid	5.6	–	–	Dina *et al.* (2012)
Cob	MAC	Methylene blue	8.0	–	–	El-Sayed *et al.* (2014)
Cob	MAC	Methylene blue	12.0	–	–	Farnane *et al.* (2018)
Cob	MAC	Methylene blue	5.6	4.0	–	Jawad *et al.* (2018)
Cob	MAC	Congo red	6.8	–	–	Leelavathy *et al.* (2015)
Cob	MAC	Methylene blue	12.0	–	–	Miyah *et al.* (2016)
Cob	MAC	Malachite green	6.0	–	–	Ojediran *et al.* (2021)
Cob	MAC	Methylene blue	7.0	–	–	Ramamoorthy *et al.* (2020)
Cob	MAC	Methylene blue	7.0	–	–	Reddy *et al.* (2016)

(*Continued.*)

Table 3 | Continued

Plant parts	Adsorbent class	Dye	Optimum pH	pHzc	Adsorption mechanism	References
Cob	MAC	Malachite green	7.0	–	–	Ismail *et al.* (2018)
Cob	MAC	Methylene blue	6.0	–	–	Tan *et al.* (2012)
Cob	MAC	Methyl orange	6.5	–	–	Wang *et al.* (2018)
Cob	MB	Methylene blue	12.0	–	–	Farnane *et al.* (2018)
Cob	MB	Malachite green	12.0	–	–	Farnane *et al.* (2018)
Cob	MB	Methylene blue	5.0	–	–	Fatoye & Onigbinde (2020)
Cob	MB	Direct blue 199	7.6	–	–	Saroj *et al.* (2015)
Cob	MBC	Methylene blue	8.0	–	–	Tsamo *et al.* (2019)
Cob	MC	Malachite green	4.0	–	–	Ong *et al.* (2017)
Cob	MC	Acid yellow	4.0	–	–	Ong *et al.* (2017)
Cover	MC	Alizarin red S	2.0	–	–	Zolgharnein *et al.* (2016)
Fibre	MAC	Alcian blue	7.0	–	–	Mallampati *et al.* (2015)
Fibre	MAC	Methylene blue	7.0	–	–	Mallampati *et al.* (2015)
Fibre	MAC	Neutral red	7.0	–	–	Mallampati *et al.* (2015)
Fibre	MAC	Coomaise brilliant blue	7.0	–	–	Mallampati *et al.* (2015)
Husk	MAC	Methylene blue	4.0	–	–	Khodaie *et al.* (2013)
Husk	MAC	Methylene blue	10.3	3.8	–	Ponce *et al.* (2021)
Husk	MB	Methylene blue	6.0	–	–	Paşka *et al.* (2014)
Husk	MC	Methylene blue	9.0	–	–	Guin *et al.* (2018)
Husk leaf	MAC	Malachite green	8.0	–	–	Jalil *et al.* (2012)
Leaves	MAC	Methyl orange	9.0	–	–	Fadhil & Eisa (2019)
Leaves	MAC	Methyl orange	9.0	–	–	Fadhil & Eisa (2019)
Leaves	MAC	Indigo carmen	12.0	–	–	Fadhil *et al.* (2021)
Leaves	MAC	Malachite green	10.0	–	–	Fadhel *et al.* (2021)
Pericarp	MAC	Methyl orange	–	11.2	–	Loya-González *et al.* (2019)
Silk	MB	Methylene blue	12.0	–	–	Miraboutalebi *et al.* (2017)
Silk	MC	Direct blue 15	3.0	–	–	Nadaroğlu *et al.* (2018)
Stalk	MAC	Methylene blue	6.0	–	–	Soldatkina & Yanar (2021)
Stalk	MAC	Malachite green	6.0	–	–	Soldatkina & Yanar (2021)
Stalk	MAC	Coomaise brilliant blue	3.0	–	–	Taha *et al.* (2021)
Stalk	MB	Malachite green	5.0	–	–	

(*Continued.*)

Table 3 | Continued

Plant parts	Adsorbent class	Dye	Optimum pH	pHzc	Adsorption mechanism	References
						Abubakar & Batagarawa (2017)
Stalk	MB	Congo red	5.0	–	–	Abubakar & Batagarawa (2017)
Stalk	MB	Malachite green	6.0	6.8	–	Lara-Vásquez *et al.* (2016)
Stalk	MB	Methylene blue	6.8	–	–	Maghri *et al.* (2012)
Stalk	MB	Coomaise brilliant blue	3.0	–	–	Taha *et al.* (2021)
Stalk + walnut shell	MAC	Malachite green	6.5	–	–	Kang *et al.* (2018)
Stalk pith	MAC	Methylene blue	10.0	–	–	Peng *et al.* (2021)
Stalk pith	MAC	Crystal violet	10.0	–	–	Peng *et al.* (2021)
Starch	MAC	Tartrazine	2.5	–	–	Dai *et al.* (2017)
Stover	MAC	Reactive red 141	3.0	–	–	Carijo *et al.* (2019)
Straw	MAC	Blue 21	2.0	–	–	Umpuch & Jutarat (2013)
Straw	MAC	Yellow 20	2.0	–	–	Umpuch & Jutarat (2013)
Straw	MB	Malachite green	6.0	2.3	–	Lima *et al.* (2017)
Straw	MB	Malachite green	6.0	–	–	Lima *et al.* (2018)
Straw	MBC	Malachite green	9.0	–	–	Eltaweil *et al.* (2020)
Straw + waste red mud	MBC	Acidic black	4.0		–	Gao *et al.* (2021)
Straw pith	MAC	Malachite green	12.0	–	–	Chen *et al.* (2020)
Straw pith	MAC	Methylene blue	12.0	–	–	Chen *et al.* (2020)
Straw pith	MAC	Rhodamine B	12.0	–	–	Chen *et al.* (2020)
Tassel powder	MAC	Reactive red 198	9.0	–	–	Dehvari *et al.* (2013)
Cob	MAC	Malachite green	12.0			Farnane *et al.* (2018)

onto maize straw adsorbent and its composite follow the pseudo-second-order kinetics that reflect chemisorption, and this conforms with most studies (Table 3) except for Muhammad *et al.* (2019), who differed in their claim and noted that chemisorption occurs through allocation electrons between cornstalk sorbent and crystal violet. Guo *et al.* (2018) further explained that based on the characterization result, the adsorbent contains numerous oxygen-containing moieties, such as OH, and hence H-bonding may participate in the adsorption course under acidic conditions, and tylosin adsorption on the adsorbents may be ascribed to hydrophobic interactions. Fathi *et al.* (2015) in their own study thermodynamically established that the negative value of ΔS^{o} implies that the adsorption process occurs via electrostatic interaction between the adsorbent surface and adsorbate molecules in the solution. Both Guo *et al.* (2018) and Fathi *et al.* (2015) also pointed out that the negative value of ΔG^{o} with the decreasing temperature makes the adsorption easier.

In addition, most reports in Table 3 empirically confirm that the amount of electrostatic charges that the dye pollutant contributes throughout the adsorption process is strongly governed by pH, and this can be easily

explained using pHzc (when the adsorbent's surface is uncharged and in other words, when there is no net charge associated with the functional group charge). For example, as the pH of the solution rises, the surface potential becomes highly negative (when pH is > pHzc), intensifying the electrostatic impact. When the pH falls below pHzc, the surface charge turns positive, making it challenging to adsorb negatively charged dye molecules (Wang & Wang 2008; Rosas-Castor *et al*. 2014; Kamarehie *et al*. 2019; Mousavi *et al*. 2021). This practical explanation is in good agreement with the one reported by Yaneva & Georgieva (2013) and Velmurugan *et al*. (2016) for the adsorption of Congo red dye, where they observed that at pH < pHzc, the surface of the unmodified and modified corn cob adsorbent was positively charged, and this was advantageous for electrostatic interactions between dye anions (negatively charged dye SO_3^- groups) and the adsorbent surface. Conversely, Yaneva & Georgieva (2013) noticed that the adsorption of the anionic dye diminished with an uptick in pH (pH 8–9), and this occurrence was linked to both the overabundance of OH ions in the solution that contend for the adsorption sites on corn cob as well as the negative charge on the surface of the adsorbent. The forgoing account is consistent with the one established by Ren *et al*. (2020), and they also added that in an acidic condition, the protonation influence of a functional group such as SO_3^- improves the electrostatic attraction between the dye and adsorbents, and as a result, the upsurge in the concentration of H^+ was advantageous for the adsorption of reactive brilliant dyes yellow and red. In another study conducted by Zhang *et al*. (2020) using corn cob biochar for the degradation of Methyl Orange (MO), it was discovered that the foundation of the oxidizing capacity of the corn cob biochar for the degradation of MO dye was taking into account the OH radical present at the biochar adsorbent surface, which vehemently struck and destroyed the N = N bond of the dye, followed by a ring-opening reaction to produce giant C_nH_{2n+2}, and final mineralization into CO_2 and H_2O molecules. It was further affirmed that electrostatic interactions, electron sharing, and electron transfer worked in concert with the radical attack to produce the MO's adsorption process (Zhang *et al*. 2020). Rosas-Castor *et al*. (2014) did not differ in their own mechanistic line of thought as well, as they suggest from their experimental findings that maize biosorbent (MB) is adsorbed predominantly on the biosorbent surface by electrostatic attraction and complexation mechanisms. Notably, as established by Barquilha & Braga (2021) and as shown in Table 3, H-bond, π–π interaction, hydrophobic interaction, and electrostatic interaction are predominant for dye adsorption. Also, as expounded by Moradi & Sharma (2021), the numerous active sites on the surface of adsorbents may be related to the charge of the dye ions as well as the active sites. The amount of adsorbed dye reduces as pH values drop because the surface charge virtually becomes positively charged, which makes cationic dye molecules more competitive with H^+. Meanwhile, for anionic dye, which can quickly bind to the adsorbent, this condition is more preferable. However, as the pH level in the system rises, a significant volume of OH ions will be released, increasing the number of negatively charged sites. A negatively charged surface affects cationic dyes in a variety of ways, but it has no effect on the adsorption of anionic dyes.

5. ADSORPTION KINETIC AND ISOTHERM MODELLING

Adsorption isotherms are generally used for describing the adsorption behaviour and evaluating the adsorption capacity of materials used for environmental remediation (Emenike *et al*. 2023; Ohale *et al*. 2023). Different adsorption models have been described in the literature to particularly monitor the uptake capacity of maize/corn adsorbents in the removal of dyes. A summary of these isotherm models and associated parameters is presented in Table 4. The practical operation of an adsorption system requires that the equilibrium data be correlated either by an empirical or theoretical equation (Iwuozor *et al*. 2022c). Many such equations abound in the open literature. However, the foregoing analysis of adsorption isotherms used to model the uptake capacity of maize/corn adsorbents showed that Freundlich and Langmuir isotherms were the most popular and frequently used isotherms used to describe the fit of the equilibrium data.

The Freundlich isotherm, which assumes that multilayer adsorption occurs through a heterogenous surface (Freundlich 1906), is mathematically expressed as follows:

$$\text{Log}\frac{X}{M} = \text{Log}\, K_f + \frac{1}{n}\text{Log}\, C_s$$

where C_s is the equilibrium concentration of the pollutant in solution (mg/L), x/m is the amount of pollutant adsorbed (mg/g), and K_f and n are Freundlich constants (Yang 1998). The two Freundlich constants are indicative of certain adsorptive interpretations; a decreased n value corresponds to an increase in surface heterogeneity

Table 4 | Best-fit isotherm and kinetic models for maize/corn adsorbents for dye uptake

			Isotherm models			Kinetic models			
Plant parts	**Adsorbent class**	**Dye**	**Best fit**	**Model type**	**R^2**	**Best fit**	**Model type**	**R^2**	**References**
Corn cob	MAC	Methylene blue	Freundlich	Linear	0.938	–	–	–	Aljeboree *et al.* (2019)
Corn stalk	MB	Malachite green	Freundlich	Linear	0.998	PSO	Linear	0.999	Abubakar & Batagarawa (2017)
Corn stalk	MB	Congo red	Langmuir	Linear	0.991	PSO	Linear	0.999	Abubakar & Batagarawa (2017)
Corn stover	MAC	Reactive red 141	Langmuir	Nonlinear	0.997	PSO	Nonlinear	0.995	Carijo *et al.* (2019)
Corn cob	MAC	Methyl violet	Freundlich	Linear	0.994	–	–	–	Aljeboree *et al.* (2021)
Corn cob	MAC	Methylene blue	Temkin	Linear	0.996	–	–	–	Aljeboree & Alkaim (2019)
Corn cob	MAC	Crystal violet	Freundlich	Linear	0.995	–	–	–	Aljeboree & Alkaim (2019)
Corn cob	MAC	Maxilone blue	Temkin	Linear	0.997	–	–	–	Aljeboree & Alkaim (2019)
Corn cob	MAC	Methylene blue	Freundlich	Linear	0.994	–	–	–	Ali *et al.* (2017)
Corn cob	MAC	Brilliant green	Freundlich	Linear	0.994	–	–	–	Ali *et al.* (2017)
Corn straw	MAC	Rhodamine B	Freundlich	Linear	0.998	PSO	Linear	0.999	Chen *et al.* (2019)
Corn cob	MB	Methylene blue	Freundlich	Linear	0.902	–	–	–	Fatoye & Onigbinde (2020)
Corn cob	MB	Methylene blue	Freundlich	Linear	0.999	PSO	Linear	0.989	Dutta & Nath (2018)
Corn cob	MAC	Methylene blue	Freundlich	Linear	0.999	PSO	Linear	0.999	Dutta & Nath (2018)
Corn cob	MAC	Methylene blue	Langmuir	Linear	0.986	–	–	–	El-Sayed *et al.* (2014)
Corn leaves	MB	Malachite green	Freundlich	Linear	0.924	PFO	Linear	0.930	Fadhel *et al.* (2021)
Corn leaves	MB	Indigo carmen	Freundlich	Linear	0.926	PSO	Linear	0.993	Fadhil *et al.* (2021)
Corn straw	MAC	Methylene blue	Temkin	Linear	0.977	PSO	Linear	0.995	Ge *et al.* (2016)
Corn stalks	MB	Direct red 23	Freundlich	Linear	0.993	PSO	Linear	0.999	Fathi *et al.* (2015)
Corn leaves	MB	Methyl orange	Freundlich	Linear	0.964	PFO	Linear	0.908	Fadhil & Eisa (2019)
Corn leaves	MAC	Methyl orange	Langmuir	Linear	0.915	PSO	Linear	0.990	Fadhil & Eisa (2019)
Corn straw	MBC	Acid black	Diffusion chemisorption model	Linear	0.972	Elovich	Linear	0.990	Gao *et al.* (2021)
Corn straw	MBC	Amino black	Diffusion chemisorption model	Linear	0.999	Elovich	Linear	0.999	Gao *et al.* (2021)
Corn cob	MB	Methylene blue	Langmuir	Linear	0.978	PSO	Linear	0.992	Farnane *et al.* (2018)
Corn cob	MB	Malachite green	Langmuir	Linear	0.941	PSO	Linear	0.983	Farnane *et al.* (2018)
Corn cob	MAC	Methylene blue	Langmuir	Linear	0.955	PSO	Linear	0.960	Farnane *et al.* (2018)
Corn cob	MAC	Malachite green	Langmuir	Linear	0.937	PSO	Linear	0.997	Farnane *et al.* (2018)

(*Continued.*)

Table 4 | Continued

Plant parts	Adsorbent class	Dye	Isotherm models			Kinetic models			References
			Best fit	Model type	R^2	Best fit	Model type	R^2	
Corn stalks	MAC	Malachite green	Langmuir	Linear	0.998	PSO	Linear	0.998	Kang *et al.* (2018)
Corn cob	MB	Gentian violet	Freundlich	Linear	0.995	PSO	Linear	1.000	Javed *et al.* (2021)
Corn cob	MAC	Methylene blue	Freundlich	Linear	0.944	PFO	Linear	0.998	Jawad *et al.* (2018)
Corn pith	MAC	Malachite green	Freundlich	Linear	0.996	PFO	Linear	0.988	Jothirani *et al.* (2016)
Corn straw	MB	Malachite green	Freundlich	Linear	0.99	Elovich	Linear	0.99	Lima *et al.* (2017)
Corn straw	MAC	Malachite green	Freundlich	Linear	0.99	Elovich	Linear	0.99	Lima *et al.* (2017)
Corn cob	MAC	Methylene blue	Langmuir	Linear	0.99	PSO	Linear	1.00	Medhat *et al.* (2021)
Corn straw	MC	Green 40	Langmuir	Linear	0.994	PSO	Linear	0.999	Umpuch (2015)

post-adsorption, while the increase in K_f is an indication of the availability of more active sites for adsorption (Ali *et al.* 2020).

On the other hand, the Langmuir isotherm describes adsorption as occurring on a homogenous surface. It posits that there is no further adsorption once an adsorbed molecule enters a site (Günay *et al.* 2007). The linear expression of the Langmuir isotherm is given as follows:

$$\frac{C_e}{q_e} = \frac{C_e}{Q_o} + \frac{1}{bQ_0}$$

where C_e is the equilibrium concentration (mg/L), q_e is the equilibrium quantity adsorbed (mg/g), and Q_O and b are adsorption efficiency constant and adsorption energy constant, respectively (Langmuir 1916).

The reviewed studies in Table 4 showed that most of the studies, regardless of adsorbent type, were better fitted to the Freundlich isotherm. The Freundlich isotherm gave a better description of the experimental data, and this was reflected in the relatively high correlation coefficients observed in the studies. However, there were cases where a particular adsorbent type was better fitted to more than one isotherm model. For instance, activated carbon of different plant parts was shown to be predominantly fitted to Freundlich and Langmuir isotherms, and sometimes to Temkin isotherm. There is another instance where the unmodified form of a plant part is fitted to Freundlich isotherm, and at other times to Langmuir isotherm. The variations exhibited by this adsorbent class could be due to variations in the adsorbate.

Adsorption kinetics provides useful information on the mass transfer mechanisms, efficiency of adsorbent used, and adsorption rate. The information provided by the adsorption kinetics is required for the design of the adsorption system (Wang & Guo 2020). There are several models of adsorption kinetics, including the Elovich model, the mixed-order model, the pseudo-first-order model, and the pseudo-second-order model, among others. The linear equations of the pseudo-first-order, pseudo-second-order, and Elovich models are presented in the following equations:

$$\mathrm{In}(q_e - q_t) = \mathrm{In}q_e - K_1 t$$

$$\frac{t}{q_t} = \frac{1}{k_2 q_e^2} + \frac{t}{q_e}$$

$$q_t = \frac{1}{b}\mathrm{In}(\mathrm{abt}) = \frac{1}{b}\mathrm{In}(\mathrm{ab}) + \frac{1}{b}\mathrm{In}(t)$$

Based on the studies reviewed, the pseudo-second-order model exhibited the best fit predominantly. However, there were cases in which the pseudo-first-order and Elovich models exhibited best fit although they had minimal frequency. It is then important to estimate the basic assumption of the pseudo-second-order model. The pseudo-second-order model assumes that the rate-limiting step of the adsorption process is chemisorption. This means that the rate of adsorption is not dependent on adsorbate concentration but on adsorption capacity (Sahoo & Prelot 2020).

6. ADSORPTION THERMODYNAMICS

The mechanism of adsorption can be further investigated by a thermodynamic process to ascertain the level of electrostatic interaction between the adsorbent and adsorbing species at a given temperature. The nature of adsorption from temperature effect variations is elucidated on the basis of adsorption enthalpy (ΔH^o), entropy (ΔS^o), and Gibbs free energy (ΔG^o). Table 5 lists the values of thermodynamic parameters that were ascertained at various temperatures from certain publications.

The physical adsorption compelled by the mode of energy interactive process, e.g., hydrogen bonding, van der Waals, and π–π interface between the adsorbent and dye pollutant, is dependent on the Gibbs free energy (ΔG^o) (Chang *et al.* 2021). A combination of negative values ($\Delta G^o < 0$) and positive values ($\Delta G^o > 0$) of Gibbs free energy at stated temperatures depicting spontaneity and non-spontaneity of chemical reactions was reported in Table 5 for several grades of adsorbent class and dye adsorbate species. The reduction in ΔG^o values with increasing temperatures of solution confirms the feasibility of thermodynamics, and the adsorption of anionic and cationic dyes is favourable at high temperatures (Chang *et al.* 2021). According to Ahmad *et al.* (2021), at increased temperature, the adsorbent pores get enlarged, subsequently initiating further activation of surface

Table 5 | Summary of thermodynamics parameters for maize/corn adsorbents for dye uptake

			Thermodynamics				
Plant parts	Adsorbent class	Dye	Temp (K)	ΔG° (kJ/mol)	ΔH° (kJ/mol)	ΔS° (J/mol·K)	References
Corn silk	MB	Reactive blue (RB19)	298	0.4765	7.70	24.22	Değermenci *et al.* (2019)
			308	0.2343			
			318	−0.0079			
			328	−0.2502			
Corn silk	MB	Reactive red (RR218)	298	1.8232	26.44	82.57	Değermenci *et al.* (2019)
			308	0.9975			
			318	0.1717			
			328	−0.6540			
Corn straw composite	MC	Malachite green	298	−8.89	40.90	167.08	Eltaweil *et al.* (2020)
			303	−9.72			
			308	−10.56			
			313	−11.39			
Corn stalk	MB	Direct red (DR23)	283.15	−4.793	57.481	228.29	Fathi *et al.* (2015)
			288.15	−5.285			
			298.15	−6.336			
			308.15	−7.394			
			318.15	−8.120			
Corn straw	MC	Methylene blue	298	−9.25	−42.66	−111.37	Ge *et al.* (2016)
			318	−7.75			
			338	−4.74			
Maize stover	MC	Methyl red	293	−5.00	7.865	0.0439	Guyo *et al.* (2017)
			303	−5.44			
			313	−5.88			
			323	−46.32			
Maize husk leaf	MC	Malachite green	303	−5.93	32.4	127	Jalil *et al.* (2012)
			313	−7.19			
			323	−8.46			
Corn cob	MBC	Methylene blue	313	−67.80	25.5	139.6	Jawad *et al.* (2018)
			323	−69.20			
			333	−70.50			
Corn straw	MB	Malachite green	298	−22.4	54.4	0.03	Lima *et al.* (2017)
			308	−25.5			
			318	−26.9			
			328	−30.6			
Corn straw	MB	Malachite green	298	−22.4	63.8	0.03	Lima *et al.* (2017)
			308	−26.3			
			318	−28.5			
			328	−31.3			
Corn straw core	MB	Methylene blue	298	−1.67	−29.95	−87.56	Liu *et al.* (2018b)
			318	−0.55			
			338	1.88			

(*Continued.*)

Table 5 | Continued

Plant parts	Adsorbent class	Dye	Thermodynamics				References
			Temp (K)	ΔG° (kJ/mol)	ΔH° (kJ/mol)	ΔS° (J/mol·K)	
Corn stalk	MB	Methylene blue	293	−26.8	9.5	124	Soldatkina & Yanar (2021)
			313	−28.9			
			333	−31.8			
Corn stalk	MB	Malachite green	293	−26.3	11.8	130	Soldatkina & Yanar (2021)
			313	−28.6			
			333	−31.5			
Corn starch	MBC	Methylene violet	298.15	−16.549	1.50	0.15	Mittal *et al.* (2018)
			308.15	−17.873			
			318.15	−19.558			
Corn cob	MAC	Methylene blue	293	−7.616	37.442	153.783	Miyah *et al.* (2016)
			303	−9.154			
			313	−10.692			
			323	−12.221			
Corn cob	MAC	Congo red	303	−32.27	−20.91	0.064	Ojedokun & Bello (2017)
			313	−34.46			
			323	−35.76			
Corn husk	MC	Methylene blue	300	−1.16	18.1	64	Guin *et al.* (2018)
			310	−1.74			
			320	−2.38			
Corn husk	MB	Methylene blue	298	−6.5651	−4.3792	15.9408	Paşka *et al.* (2014)
			313	−6.5755			
			333	−5.6497			
Corn straw	MAC	Reactive brilliant yellow	298	−7.05	1.61	29.05	Ren *et al.* (2020)
			308	−7.34			
			318	−7.63			
Corn straw	MAC	Reactive brilliant red	298	−7.08	1.41	28.47	Ren *et al.* (2020)
			308	−7.36			
			318	−7.65			
Maize cob	MB	Bromophenol blue	298	−5.039	−4.226	0.003	Abubakar & Ibrahim (2018)
			303	−5.052			
			308	−5.066			
			313	−5.079			
			318	−5.093			
Maize cob	MB	Bromothymol blue	298	−1.528	6.871	0.028	Abubakar & Ibrahim (2018)
			303	−1.669			
			308	−1.810			
			313	−1.951			
			318	−2.092			

(*Continued.*)

Table 5 | Continued

Plant parts	Adsorbent class	Dye	Thermodynamics				References
			Temp (K)	ΔG° (kJ/mol)	ΔH° (kJ/mol)	ΔS° (J/mol·K)	
Corn cob leaves	MB	Basic violet 4	303	−12.57	−14.43	−0.0061	Sepúlveda *et al.* (2015)
			318	−12.47			
			333	−12.38			
Corn stalk	MB	Acidic red	303	−30.2	−9.0	70	Soldatkina & Zavrichko (2018)
			318	−31.3			
			328	−31.9			
Corn stalk	MB	Acidic orange	303	−30.0	−14.0	53	Soldatkina & Zavrichko (2018)
			318	−31.2			
			328	−31.3			
Maize cob	MBC	Methylene blue	298	−1.44	−11.908	−0.037	Tsamo *et al.* (2019)
			303	0.23			
			318	−0.36			
			333	0.41			
Corn stalk	MC	Methylene blue	303.15	−4.956	−21.471	−0.054	Wen *et al.* (2018)
			313.15	−4.454			
			323.15	−3.817			
			333.15	−3.353			
Corn cover	MC	Alizarin red S	298	−1.51	−2.81	−4.6	Zolgharnein *et al.* (2016)
Corn stover	MC	Indigo carmine	288	−23,485	2.914	491.4	Ahmad *et al.* (2021)
			298	−26,770			
			308	−28,478			
			318	−29,572			

sites, leading to a decrease in ΔG^{o}. On the contrary, Wen *et al.* (2018) reported a rise in negative values of ΔG^{o} at decreased temperatures that recorded advantageous adsorption processes, and this could be enhanced mobility of the cationic dye at higher temperatures, thereby producing lower adsorption capacity. The positive and negative values of ΔH^{o} observed in Table 5 show that the sorption mechanism is either endothermic or exothermic in nature, in corroboration with the effect of temperature. The exothermic reaction from dye biosorption onto the maize biomass surface site also indicates the existence of a chemical interaction between the adsorbing species and the adsorbate, whereas in the case of the endothermic process, the biosorption is physisorption, indicating a weak interaction between the maize biomass and dye types (Mbarki *et al.* 2018). The positive values of ΔH^{o} observed in the reviewed literature could be due to probable structural deformation and inducement of a photocatalytic effect by specific functional groups of the maize biomass adsorbent in the adsorption system (Chang *et al.* 2021).

Entropy change (ΔS^{o}) is a parameter for evaluating the magnitude of irregularity between the adsorbate molecules and the adsorbent. The positive value of ΔS^{o} for the adsorption dyes on different active sites of the adsorbent class designates a rise in sorption randomness, and the attraction of the adsorbent for the dye molecules was high (Soldatkina & Zavrichko 2018). The increase in randomness at the solid–solution interface throughout the adsorption process is indicated by the positive change in entropy values in several prior studies (Table 5). The kinetic energy of the adsorbate molecules rises as a result of the mobility of dye molecules on the sorbent surface site increasing with the temperature increase at positive values of entropy change. On the other hand, the negative values of ΔS^{o} in dye adsorption on composite and improved corn straw elucidate a decrease in the degree of disorderliness between the dye molecules and corn adsorbent class (Ge *et al.* 2016; Liu *et al.* 2018b).

Similar inferences were observed in the adsorption of dye species on UM cob (Sepúlveda *et al.* 2015), maize cob biochar (Tsamo *et al.* 2019), composite corn stalk (Wen *et al.* 2018), and composite corn cover (Zolgharnein *et al.* 2016), as shown in Table 5, which could be attributed to the loss of at least a degree of freedom by dye molecules when adsorbed and no occurrence of a notable change in entropy (Wen *et al.* 2018).

7. REGENERATION AND REUSABILITY STUDIES

The practical utilization of any adsorbent is predicated upon its potential for use multiple times (Emenike *et al.* 2022c). However, not many studies have attempted to investigate the possibility of regenerating and reusing maize/corn adsorbents in the adsorption of dyes. Nevertheless, an overview of the studies that carried out this is presented in Table 6. There were significant variations in desorption of the dyes. There were cases where the regeneration efficiencies were higher than 100% after two desorptions, even when the use of two different eluents (NaCl and HCl) was employed. In the study, this observation was attributed to a possible reaction between the lone pair of electrons on the adsorbent and the H^+ on the HCl eluent, thus leading to the availability of more reaction sites for the removal of dyes (Song *et al.* 2016). In some instances, the use of the same eluent exhibited varying regeneration efficiencies, although they were used in the removal of different dyes. Similarly, while some adsorbents performed over long, repeated cycles, others could only be reused once. Hence, it suffices to say that the regenerative efficiency of an adsorbent would depend on the adsorbent type (unmodified or modified), the eluent used, and the pollutant to be removed from the environmental matrix.

8. COMPETITIVE ADSORPTION

Competitive adsorption explains the level of adsorbent attraction to the dye adsorbate ions in the presence of other existing competing chemical ions in aqueous media. In some textile industries, several electrolytes are added to the dye solution to increase the dye's fastness on the fabrics, thereby accumulating inorganic salts in the effluents that may disrupt the adsorption performance at given concentrations (Peng *et al.* 2021). Again, the nature of modified or activated biosorbent can introduce coexisting ions during the sorption process, which can compete with dye contaminants for the sorption sites, which may either increase or decrease the ionic strength. The effect of ionic strength on the adsorption tendency of corn stigmata biomass for cationic (methylene blue) and anionic (indigo carmine) dyes was analysed using NaCl solution at varying concentrations of 10, 100, and 1,000 mM (Mbarki *et al.* 2018). It was observed that the adsorption capacity of methylene blue decreased from 8.267 to 5.972 mg/g and from 8.036 to 1.307 mg/g for indigo carmine at increased concentrations. The positive effect of the salt on the decreased biosorption capacity of methylene blue dye could be due to the competitive interaction between Na^+ and cationic dye on the biomass negative surface sites. In addition, the impact of Cl^- of salt on the adsorption of indigo carmine follows similar competition between the chloride ion and anionic dye, SO_3^-, on the modified sorbent attracting sites.

The adsorption behaviour of a magnetic carbonaceous-prepared adsorbent from corn starch in dye aqueous solutions comprising NaCl and $CaCl_2$ was investigated to evaluate the binding interaction between the carbonized adsorbent and methylene violet dye (Mittal *et al.* 2018). A decrease in efficiency of adsorption was observed with increasing concentrations of cations (0.1, 0.2, 0.3, 0.4, 0.5, and 0.6 M) in the dye solution, which depicts possible competitive electrostatic contacts between the cationic dye molecules and cations (Na^+ and Ca^{2+}) on the negatively charged binding sites of the carbonaceous adsorbent material. The existence of Ca^{2+} in the organic dye solution reduces the adsorption capacity more effectively than Na^+ as a result of the smaller hydrated radius of the calcium ion, which aids its mobility in an aqueous solution and has a stronger competing tendency than monovalent ions. Furthermore, the result of coexisting cations (H^+ and K^+) on the sorption performance of H_3PO_4-modified corn stalk for methylene blue dye was reported by Tang *et al.* (2019). The uptake efficiency of methylene blue by the modified adsorbent decreased in the presence of increasing H^+ and K^+ ion concentrations, which showed that partial displacement and ion exchange were involved during the adsorption mechanism. H^+ displayed lower adsorption capacity owing to higher attraction to adsorption sites with a reduced hydrated radius (2.83 Å) than K^+, and hence, the driving force for the uptake was highly involved. Tang *et al.* (2021) reported on the competing effect of varying concentrations of K^+ and Ca^{2+} on the adsorption capacity of carboxylate-modified corn stalk for methylene blue dye. The adsorption capacity values of methylene blue were reduced in the presence of K^+ and Ca^{2+} ions with concentrations ranging from 0 to 0.03 mol/L, (Table 7) thus indicating competition with the organic dye-attracting active site on the treated

Table 6 | Desorption/reuse studies for dye uptake by maize/corn adsorbents

Plant parts	Adsorbent class	Dye	Eluent	Number of cycles (n)	% desorbed ($n = 1$)	% q_m retained after n cycles	References
Corn stalk	MAC	Methylene blue	Deionized water	1	75	–	Mousavi *et al.* (2020)
Corn stalk	MAC	Malachite green	–	5	90.2	33.65	Kang *et al.* (2018)
Corn starch	MAC	Methylene blue	Acetone	20	100	–	Mittal *et al.* (2020)
Corn stalk	MC	Methyl orange	NaCl	3	–	–	Song *et al.* (2016)
Corn cob	MBC	Methyl orange	–	3	> 99	–	Zhang *et al.* (2020)
Corn starch	MC	Golden yellow X-GL	Ethanol	4	≤ 85	–	Guo *et al.* (2019)
Corn straw	MC	Methylene blue	Hydrochloric acid	5	80.6	–	Liu *et al.* (2020b)
Corn fibers	MB	Alcian blue	Acid and alkali solutions	5	96	–	Mallampati *et al.* (2015)
Corn fibers	MB	Methylene blue	Acid and alkali solutions	5	96	–	Mallampati *et al.* (2015)
Corn fibers	MB	Coomassie brilliant blue	Acid and alkali solutions	5	96	–	Mallampati *et al.* (2015)
Corn fibers	MB	Neutral red	Acid and alkali solutions	5	96	–	Mallampati *et al.* (2015)
Corn stover	MC	Reactive red 141	NaOH	–	< 12	–	Carijo *et al.* (2019)
Corn stover	MC	Reactive red 141	NaCl	–	< 12	–	Carijo *et al.* (2019)
Corn stover	MC	Reactive red 141	KOH	–	< 12	–	Carijo *et al.* (2019)
Corn stover	MC	Reactive red 141	Ethanol	–	< 12	–	Carijo *et al.* (2019)
Corn stover	MC	Reactive red 141	hexane	–	< 12	–	Carijo *et al.* (2019)
Corn pericarp	MB	Methylene blue	Deionized water	7	≤ 5	–	Rosas-Castor *et al.* (2014)
Corn pericarp	MB	Methylene blue	Hydrochloric acid	7	≤ 70	–	Rosas-Castor *et al.* (2014)
Corn pericarp	MB	Methylene blue	Ethanol	7	≤ 30	–	Rosas-Castor *et al.* (2014)
Corn pericarp	MB	Methylene blue	NaOH	7	≤ 5	–	Rosas-Castor *et al.* (2014)
Corn straw	MC	Methylene blue	Ethanol	4	70–90	–	Zhao *et al.* (2014)
Corn cob	MB	Gentian violet	KOH	–	92.5	–	Javed *et al.* (2021)

Table 7 | Competitive adsorption study for dye uptake by maize/corn adsorbents

Plant parts	Adsorbent class	Dye	Competing species	Concentration of competing species	Maximum change with competing species	References
Corn stigmata	MB	Methylene blue	NaCl	1,000 mM	27.76% decrease	Mbarki *et al.* (2018)
Corn stigmata	MB	Indigo carmine	NaCl	1,000 mM	83.74% decrease	Mbarki *et al.* (2018)
Corn starch	MBC	Methylene violet	CaCl	0.6 M	23% decrease	Mittal *et al.* (2018)
Corn starch	MBC	Methylene violet	NaCl	0.6 M	20.5% decrease	Mittal *et al.* (2018)
Corn stalk	MB	Methylene blue	H^+	0.02 mol/L	71% decrease	Tang *et al.* (2019)
Corn stalk	MB	Methylene blue	K^+	0.04 mol/L	16% decrease	Tang *et al.* (2019)
Corn stalk	MB	Methylene blue	K^+	0.030 mol/L	35.71% decrease	Tang *et al.* (2021)
Corn stalk	MB	Methylene blue	Ca^{2+}	0.030 mol/L	85.71% decrease	Tang *et al.* (2021)
Corn stalk pith	MB	Crystal violet	NaCl	0.02 mol/L	30.65% decrease	Peng *et al.* (2021)
Corn stalk pith	MB	Methylene blue	NaCl	0.02 mol/L	57.58% decrease	Tang *et al.* (2019)

adsorbent. The competing behaviour of Ca^{2+} decreased the removal efficiency of dye pollutants compared to K^+ as a result of the smaller ionic radius of Ca^{2+}, which constitutes a driving force for easier attraction of the sorption sites. The study further stated that the cations competed with the dye at lower coexisting concentrations, generating a highly decreased range of adsorption capacity, whereas at increasing concentrations, the electrostatic connections between the dye molecule and the surface sites are being inhibited by K^+ and Ca^{2+}. The effect of inorganic anions (Cl^-, NO_2^-, NO_3^-, SO_4^{2-}, and HPO_4^{2-}) on the removal performance of cationic dyes (methylene blue and crystal violet) on corn pith biosorbent at concentrations of 0.05 M was evaluated (Peng *et al.* 2021). It was noted that the sorption efficiency for single and binary cationic dye molecule solutions was somewhat reduced in the presence of varied sodium salts. The status of adsorption inhibition by the anions in a single methylene blue dye aqueous solution follows this order: $SO_4^{2-} > HPO_4^{2-} > Cl^- > NO_2^- > NO_3^-$, showing stronger competition of divalent electrolytes (Na_2SO_4 and Na_2HPO_4) with the dye molecules for limited adsorption sites than monovalent anions. The adsorption capacity of corn pith biosorbent decreased considerably for both sole and binary dye solutions, with a reduction in ionic strength at increased salt concentrations. This is due to the incessant competing electrostatic interaction that existed between Na^+ and dye molecules for activated active sites, leading to an increased inhibitory effect on dye removal. In general, the reduction in sorption efficiency of maize biomass for organic dyes is a result of the compressibility of the adsorbent double layer caused by increased ionic strength, thus reducing the electrostatic attraction between the pollutant species and prepared corn biomass.

9. FINDINGS AND FUTURE PROSPECTS

The adsorption behaviour of a variety of dyes on corn/maize-based materials was reviewed in this study. From the available data, the most utilized corn biomass was cob, stalk, and straw, followed by husk, silk, and leaves. The adsorbents were grouped into four classes, namely, biosorbents, activated carbons, biochar, and composites. All the forms of corn/maize-based adsorbents exhibited high adsorption performance relative to the pre-treated precursor. This was due to the development of porous structure, functionality, and elemental composition in the modified or treated material. In particular, corn/maize-based composites and activated carbon adsorbents showed high surface areas with favourable functionality, which improved adsorbent's efficacy. The maximum uptake of dye was 1,682 mg/g for methylene blue using corn husk-based composite adsorbent, followed by

Rhodamine B (using corn/maize-based activated carbon) with an adsorption capacity of 1,578 mg/g. Freundlich and pseudo-second-order models best represented the isotherm and kinetic data of the adsorbents for a variety of dyes. Freundlich and PFO models were also applicable in some studies. The parameters of the Langmuir and Freundlich isotherm models confirm the favourable adsorption nature. The main mechanisms for studied adsorption systems involve electrostatic attraction, ion exchange, and hydrogen bonding, along with complexation, pore filling, and π–π interaction. Thermodynamic results confirm spontaneous, endothermic/exothermic, and feasible adsorption natures.

Corn/maize-based materials were extensively addressed in the literature as highly efficient adsorbents for aquatic contaminants. Nevertheless, some points still need to be considered. Futuristic studies should consider applying two or more corn residues as precursors for adsorbent production. In addition, studies should also include the optimization of preparation variables for the corn/maize materials. There is also a need to test the behaviour of binary or multiple dye adsorbate systems as obtained in industrial wastewaters. Also, identifying the efficiency of corn-based materials for eliminating actual effluents in a continuous adsorption unit could be delved into. Furthermore, there is a need for cost analysis studies. Cost is an important factor in the choice of an adsorbent for industry. Cost analysis studies will not only help industries make informed and feasible decisions but also help futuristic works in this field of study and allow for comparison with commercial adsorbents.

COMPLIANCE WITH ETHICAL STANDARDS

This article does not contain any studies involving human or animal subjects.

FUNDING

There was no external funding for the study.

AUTHORS CONTRIBUTIONS

Kingsley O. Iwuozor: conceptualization, methodology, data curation, writing – original draft, writing – review and editing, validation. Chisom T. Umeh: data curation, writing – original draft, writing – review and editing, validation. Stephen Sunday Emmanuel: data curation, writing – original draft, writing – review and editing, validation. Ebuka Chizitere Emenike: methodology, data curation, writing – original draft, writing – review and editing, validation. Abel U. Egbemhenghe: writing – original draft and writing – review & editing. Odunayo T. Ore: writing – original draft and writing – review and editing. Taiwo Temitayo Micheal: data curation, writing – original draft, writing – review and editing, validation. Fredrick O. Omoarukhe: writing – original draft; writing – review & editing. Patience A. Sagboye; data curation, writing – original draft, writing – review and editing, validation. Victor E. Ojukwu: writing – original draft and writing – review and editing. Adewale George Adeniyi: conceptualization, methodology, writing – original draft; writing – review and editing, validation, supervision, project administration.

DATA AVAILABILITY STATEMENT

All relevant data are included in the paper or its Supplementary Information.

CONFLICT OF INTEREST

The authors declare there is no conflict.

REFERENCES

Abdel-Aal, S., Gad, Y. & Dessouki, A. 2006 Use of rice straw and radiation-modified maize starch/acrylonitrile in the treatment of wastewater. *Journal of Hazardous Materials* **129**(1–3), 204–215.

Abdelwahab, O. 2008 Evaluation of the use of loofa activated carbons as potential adsorbents for aqueous solutions containing dye. *Desalination* **222**(1), 357–367. https://doi.org/10.1016/j.desal.2007.01.146.

Abdullah, N. H., Ghani, N. A. A., Razab, M. K. A. A., Noor, A. a. M., Halim, A. Z. A., Rasat, M. S. M., Wong, K. N. S. W. S. & Amin, M. F. M. 2019 Methyl orange adsorption from aqueous solution by corn cob based activated carbon. In: *AIP Conference Proceedings*. 18–19 August, 2018, Kelantan, Malaysia. AIP Publishing LLC.

Abubakar, A. & Batagarawa, S. M. 2017 Kinetic and isotherm studies of malachite green and Congo red adsorption from aqueous solution by corn stalk bio-waste material. *Bayero Journal of Pure and Applied Sciences* **10**(1), 350–355.

Abubakar, S. I. & Ibrahim, M. B. 2018 Adsorption of bromophenol blue and bromothymol blue dyes onto raw maize cob. *Bayero Journal of Pure and Applied Sciences* **11**(1), 273–281.

Adeniyi, A. G., Emenike, E. C., Iwuozor, K. O., Okoro, H. K. & Ige, O. O. 2022 Acid mine drainage: The footprint of the Nigeria mining industry. *Chemistry Africa* **5**, 1907–1920. https://doi.org/10.1007/s42250-022-00493-3.

Ahmad, A., Khan, N., Giri, B. S., Chowdhary, P. & Chaturvedi, P. 2020 Removal of methylene blue dye using rice husk, cow dung and sludge biochar: Characterization, application, and kinetic studies. *Bioresource Technology* **306**, 123202.

Ahmad, M. B., Soomro, U., Muqeet, M. & Ahmed, Z. 2021 Adsorption of Indigo Carmine dye onto the surface-modified adsorbent prepared from municipal waste and simulation using deep neural network. *Journal of Hazardous Materials* **408**, 124433.

Ali, A. F., Kovo, A. S. & Adetunji, S. A. 2017 Methylene blue and brilliant green dyes removal from aqueous solution using agricultural wastes activated carbon. *Journal of Encapsulation and Adsorption Sciences* **7**(2), 95–107.

Ali, F., Ali, N., Bibi, I., Said, A., Nawaz, S., Ali, Z., Salman, S. M., Iqbal, H. M. & Bilal, M. 2020 Adsorption isotherm, kinetics and thermodynamic of acid blue and basic blue dyes onto activated charcoal. *Case Studies in Chemical and Environmental Engineering* **2**, 100040.

Aljeboree, A. M. & Alkaim, A. F. 2019 Comparative removal of three textile dyes from aqueous solutions by adsorption: As a model (corn-cob source waste) of plants role in environmental enhancement. *Plant Archives* **19**(1), 1613–1620.

Aljeboree, A. M., Hussein, F. H. & Alkaim, A. F. 2019 Removal of textile dye (methylene blue MB) from aqueous solution by activated carbon as a model (corn-cob source waste of plant): As a model of environmental enhancement. *Plant Archives* **19**(2), 906–909.

Aljeboree, A. M., Al-Baitai, A. Y., Abdalhadi, S. M. & Alkaim, A. F. 2021 Investigation study of removing methyl violet dye from aqueous solutions using corn-cob as a source of activated carbon. *Egyptian Journal of Chemistry* **64**(6), 2873–2878.

Al-Swaidan, H. M. & Ahmad, A. 2011 Synthesis and characterization of activated carbon from Saudi Arabian dates tree's fronds wastes. In 3rd International Conference on Chemical, Biological and Environmental Engineering, 23–25 September, 2011, Singapore.

Arquilada, A. M., Ilano, C. J., Pineda, P., Felicita, J. M. & Cid-Andres, A. 2018 Adsorption studies of heavy metals and dyes using corn cob: A review. *Global Scientific Journals* **6**(12), 343–376.

Assirey, E. A. & Altamimi, L. R. 2021 Chemical analysis of corn cob-based biochar and its role as water decontaminants. *Journal of Taibah University for Science* **15**(1), 111–121.

Balathanigaimani, M., Shim, W.-G., Park, K. H., Lee, J.-W. & Moon, H. 2009 Effects of structural and surface energetic heterogeneity properties of novel corn grain-based activated carbons on dye adsorption. *Microporous and Mesoporous Materials* **118**(1–3), 232–238.

Barquilha, C. E. & Braga, M. C. 2021 Adsorption of organic and inorganic pollutants onto biochars: Challenges, operating conditions, and mechanisms. *Bioresource Technology Reports* **15**, 100728.

Bello, O. S. & Ahmad, M. A. 2011 Adsorption of dyes from aqueous solution using chemical activated mango peels. In: 2nd International Conference on Environmental Science and Technology (ICEST), September, 2016, Belgrade, Serbia.

Billa, S. F., Angwafo, T. E. & Ngome, A. F. 2019 Agro-environmental characterization of biochar issued from crop wastes in the humid forest zone of Cameroon. *International Journal of Recycling of Organic Waste in Agriculture* **8**(1), 1–13.

Budinova, T., Ekinci, E., Yardim, F., Grimm, A., Björnbom, E., Minkova, V. & Goranova, M. 2006 Characterization and application of activated carbon produced by H3PO4 and water vapor activation. *Fuel Processing Technology* **87**(10), 899–905.

Campbell, Q., Bunt, J., Kasaini, H. & Kruger, D. 2012 The preparation of activated carbon from South African coal. *Journal of the Southern African Institute of Mining and Metallurgy* **112**(1), 37–44.

Campos, N. F., Guedes, G. A., Oliveira, L. P., Gama, B. M., Sales, D. C., Rodriguez-Diaz, J. M., Barbosa, C. M. & Duarte, M. M. 2020 Competitive adsorption between Cu2+ and Ni2+ on corn cob activated carbon and the difference of thermal effects on mono and bicomponent systems. *Journal of Environmental Chemical Engineering* **8**(5), 104232.

Carijo, P. M., Dos Reis, G. S., Lima, É. C., Oliveira, M. L. & Dotto, G. L. 2019 Functionalization of corn stover with 3-aminopropyltrietoxysilane to uptake reactive Red 141 from aqueous solutions. *Environmental Science and Pollution Research* **26**(31), 32198–32208.

Chang, B. P., Gupta, A. & Mekonnen, T. H. 2021 Flame synthesis of carbon nanoparticles from corn oil as a highly effective cationic dye adsorbent. *Chemosphere* **282**, 131062. https://doi.org/10.1016/j.chemosphere.2021.131062.

Chen, S., Yue, Q., Gao, B., Li, Q. & Xu, X. 2011 Removal of Cr (VI) from aqueous solution using modified corn stalks: Characteristic, equilibrium, kinetic and thermodynamic study. *Chemical Engineering Journal* **168**(2), 909–917.

Chen, S., Yue, Q., Gao, B., Li, Q., Xu, X. & Fu, K. 2012 Adsorption of hexavalent chromium from aqueous solution by modified corn stalk: A fixed-bed column study. *Bioresource Technology* **113**, 114–120.

Chen, S., Chen, G., Chen, H., Sun, Y., Yu, X., Su, Y. & Tang, S. 2019 Preparation of porous carbon-based material from corn straw via mixed alkali and its application for removal of dye. *Colloids and Surfaces A: Physicochemical and Engineering Aspects* **568**, 173–183.

Chen, J., Liu, S., Ge, H. & Zou, Y. 2020 A hydrophobic bio-adsorbent synthesized by nanoparticle-modified graphene oxide coated corn straw pith for dye adsorption and photocatalytic degradation. *Environmental Technology* **41**(27), 3633–3645.

Crini, G. 2005 Recent developments in polysaccharide-based materials used as adsorbents in wastewater treatment. *Progress in Polymer Science* **30**(1), 38–70.

Crini, G., Lichtfouse, E., Wilson, L. D. & Morin-Crini, N. 2019 Conventional and non-conventional adsorbents for wastewater treatment. *Environmental Chemistry Letters* **17**(1), 195–213. doi:10.1007/s10311-018-0786-8.

Cruz, G., Pirilä, M., Huuhtanen, M., Carrión, L., Alvarenga, E. & Keiski, R. L. 2012 Production of activated carbon from cocoa (*Theobroma cacao*) pod husk. *Journal of Civil and Environmental Engineering* **2**(2), 1–6.

Dada, A. O., Inyinbor, A. & Oluyori, A. 2012 Comparative adsorption of dyes unto activated carbon prepared from maize stems and sugar cane stems. *Comparative Adsorption of Dyes Unto Activated Carbon Prepared From Maize Stems and Sugar Cane Stems* **2**(3), 38–43.

Dai, R., Woo, M. W., Chen, H., Dang, X., Mansouri, S. & Shan, Z. 2017 Hydrogel beads based on oxidized corn starch cross-linked with gelatin for tartrazine adsorption from aqueous environments. *Polymer Journal* **49**(7), 549–555.

Danish, M., Hashim, R., Ibrahim, M. M., Rafatullah, M., Ahmad, T. & Sulaiman, O. 2011 Characterization of *Acacia mangium* wood based activated carbons prepared in the presence of basic activating agents. *BioResources* **6**(3), 3019–3033.

Değermenci, G. D., Değermenci, N., Ayvaoğlu, V., Durmaz, E., Çakır, D. & Akan, E. 2019 Adsorption of reactive dyes on lignocellulosic waste; characterization, equilibrium, kinetic and thermodynamic studies. *Journal of Cleaner Production* **225**, 1220–1229.

Dehkhoda, A. M., Ellis, N. & Gyenge, E. 2016 Effect of activated biochar porous structure on the capacitive deionization of NaCl and zncl2 solutions. *Microporous and Mesoporous Materials* **224**, 217–228.

Dehvari, M., Ghaneian, M. T., Fallah, F., Sahraee, M. & Jamshidi, B. 2013 Evaluation of maize tassel powder efficiency in removal of reactive red 198 dye from synthetic textile wastewater. *Journal of Community Health Research* **1**(3), 153–165.

Dina, D., Ntieche, A., Ndi, J. & Ketcha Mbadcam, J. 2012 Adsorption of acetic acid onto activated carbons obtained from maize cobs by chemical activation with zinc chloride ($ZnCl_2$). *Research Journal of Chemical Sciences* **2231**, 606X.

Duru, C. E. & Duru, I. A. 2017 Adsorption capacity of maize biomass parts in the remediation of Cu2+ ion polluted water. *World News of Natural Sciences* **12**, 51–62.

Duru, C., Duru, I., Ogbonna, C., Enedoh, M. & Emele, P. 2019 Adsorption of copper ions from aqueous solution onto natural and pretreated maize husk: Adsorption efficiency and kinetic studies. *Journal of Chemical Society of Nigeria* **44**(5), 798–803.

Dutta, D. P. & Nath, S. 2018 Low cost synthesis of SiO_2/C nanocomposite from corn cobs and its adsorption of uranium (VI), chromium (VI) and cationic dyes from wastewater. *Journal of Molecular Liquids* **269**, 140–151.

Ekpete, O. & Horsfall, M. 2011 Preparation and characterization of activated carbon derived from fluted pumpkin stem waste (*Telfairia occidentalis* Hook F). *Research Journal of Chemical Sciences* **1**(3), 10–17.

El-Bendary, N., El-Etriby, H. K. & Mahanna, H. 2021 High performance removal of iron from aqueous solution using modified activated carbon prepared from corn cobs and luffa sponge. *Desalin Water Treat* **213**, 348–357.

El-Sayed, G. O., Yehia, M. M. & Asaad, A. A. 2014 Assessment of activated carbon prepared from corncob by chemical activation with phosphoric acid. *Water Resources and Industry* **7**, 66–75.

Eltaweil, A., Mohamed, H. A., Abd El-Monaem, E. M. & El-Subruiti, G. 2020 Mesoporous magnetic biochar composite for enhanced adsorption of malachite green dye: Characterization, adsorption kinetics, thermodynamics and isotherms. *Advanced Powder Technology* **31**(3), 1253–1263.

Emenike, E. C., Iwuozor, K. O. & Anidiobi, S. U. 2021 Heavy metal pollution in aquaculture: Sources, impacts and mitigation techniques. *Biological Trace Element Research* **200**, 4476–4492.

Emenike, E. C., Adeniyi, A. G., Omuku, P. E., Okwu, K. C. & Iwuozor, K. O. 2022a Recent advances in nano-adsorbents for the sequestration of copper from water. *Journal of Water Process Engineering* **47**, 102715.

Emenike, E. C., Ogunniyi, S., Ighalo, J. O., Iwuozor, K. O., Okoro, H. K. & Adeniyi, A. G. 2022b Delonix regia biochar potential in removing phenol from industrial wastewater. *Bioresource Technology Reports* **19**, 101195.

Emenike, E. C., Adeleke, J., Iwuozor, K. O., Ogunniyi, S., Adeyanju, C. A., Amusa, V. T., Okoro, H. K. & Adeniyi, A. G. 2022c Adsorption of crude oil from aqueous solution: A review. *Journal of Water Process Engineering* **50**, 103330.

Emenike, E. C., Adeniyi, A. G., Iwuozor, K. O., Okorie, C. J., Egbemhenghe, A. U., Omuku, P. E., Okwu, K. C. & Saliu, O. D. 2023 A critical review on the removal of mercury (Hg2+) from aqueous solution using nanoadsorbents. *Environmental Nanotechnology, Monitoring & Management* **20**, 100816. https://doi.org/10.1016/j.enmm.2023.100816.

Emmanuel, S. S. & Adesibikan, A. A. 2021 Bio-fabricated green silver nano-architecture for degradation of methylene blue water contaminant: A mini-review. *Water Environment Research* **93**(12), 2873–2882.

Emmanuel, S. S., Adesibikan, A. A. & Saliu, O. D. 2023a Phytogenically bioengineered metal nanoarchitecture for degradation of refractory dye water pollutants: A pragmatic minireview. *Applied Organometallic Chemistry* **37**(2), e6946. https://doi.org/10.1002/aoc.6946.

Emmanuel, S. S., Adesibikan, A. A., Saliu, O. D. & Opatola, E. A. 2023b Greenly biosynthesized bimetallic nanoparticles for ecofriendly degradation of notorious dye pollutants: A review. *Plant Nano Biology* **3**, 100024. https://doi.org/10.1016/j.plana.2023.100024.

Fadhel, O. H., Eisa, M. Y. & Zair, Z. R. 2021 Decolorizing of malachite green dye by adsorption using corn leaves as adsorbent material. *Journal of Engineering* **27**(2), 1–12.

Fadhil, O. H. & Eisa, M. Y. 2019 Removal of methyl orange from aqueous solutions by adsorption using corn leaves as adsorbent material. *Journal of Engineering* **25**(4), 55–69.

Fadhil, O. H. F. H., Eisa, M. Y., Salih, D. A. & Nafeaa, Z. R. 2021 Adsorption of Indigo Carmen dye by using corn leaves as natural adsorbent material. *Al-Khwarizmi Engineering Journal* **17**(1), 43–50.

Farnane, M., Tounsadi, H., Machrouhi, A., Elhalil, A., Mahjoubi, F., Sadiq, M., Abdennouri, M., Qourzal, S. & Barka, N. 2018 Dye removal from aqueous solution by raw maize corncob and H_3PO_4 activated maize corncob. *Journal of Water Reuse and Desalination* **8**(2), 214–224.

Fathi, M., Asfaram, A. & Farhangi, A. 2015 Removal of Direct Red 23 from aqueous solution using corn stalks: Isotherms, kinetics and thermodynamic studies. *Spectrochimica Acta Part A: Molecular and Biomolecular Spectroscopy* **135**, 364–372.

Fatoye, E. & Onigbinde, M. 2020 Dye adsorption with sugarcane bagasse and corn cob. *SAU Science-Tech Journal* **5**(1), 182–193.

Freundlich, H. 1906 Over the adsorption in solution. *The Journal of Physical Chemistry* **57**(385471), 1100–1107.

Gao, Y., Jiang, Z., Li, J., Xie, W., Jiang, Q., Bi, M. & Zhang, Y. 2019 A comparison of the characteristics and atrazine adsorption capacity of co-pyrolysed and mixed biochars generated from corn straw and sawdust. *Environmental Research* **172**, 561–568.

Gao, Y., Zhang, J., Chen, C., Du, Y., Teng, G. & Wu, Z. 2021 Functional biochar fabricated from waste red mud and corn straw in China for acidic dye wastewater treatment. *Journal of Cleaner Production* **320**, 128887.

Ge, H., Wang, C., Liu, S. & Huang, Z. 2016 Synthesis of citric acid functionalized magnetic graphene oxide coated corn straw for methylene blue adsorption. *Bioresource Technology* **221**, 419–429.

Ghasemi, S. M., Mohseni-Bandpei, A., Ghaderpoori, M., Fakhri, Y., Keramati, H., Taghavi, M., Moradi, B. & Karimyan, K. 2017 Application of modified maize hull for removal of Cu (II) ions from aqueous solutions. *Environment Protection Engineering* **43**(4), 93–103.

Giraldo, L. & Moreno-Piraján, J. C. 2012 Synthesis of activated carbon mesoporous from coffee waste and its application in adsorption zinc and mercury ions from aqueous solution. *E-Journal of Chemistry* **9**(2), 938–948.

Gong, J., Wang, X., Shao, X., Yuan, S., Yang, C. & Hu, X. 2012 Adsorption of heavy metal ions by hierarchically structured magnetite-carbonaceous spheres. *Talanta* **101**, 45–52.

Guin, J. P., Bhardwaj, Y. & Varshney, L. 2018 Radiation grafting: A voyage from bio-waste corn husk to an efficient thermostable adsorbent. *Carbohydrate Polymers* **183**, 151–164.

Günay, A., Arslankaya, E. & Tosun, I. 2007 Lead removal from aqueous solution by natural and pretreated clinoptilolite: Adsorption equilibrium and kinetics. *Journal of Hazardous Materials* **146**(1–2), 362–371.

Guo, H., Zhang, S., Kou, Z., Zhai, S., Ma, W. & Yang, Y. 2015a Removal of cadmium (II) from aqueous solutions by chemically modified maize straw. *Carbohydrate Polymers* **115**, 177–185.

Guo, L., Liu, R., Li, X., Sun, Y. & Du, X. 2015b The physical and adsorption properties of different modified corn starches. *Starch-Stärke* **67**(3–4), 237–246.

Guo, X., Yin, Y., Yang, C. & Dang, Z. 2018 Maize straw decorated with sulfide for tylosin removal from the water. *Ecotoxicology and Environmental Safety* **152**, 16–23.

Guo, J., Wang, J., Zheng, G. & Jiang, X. 2019 A TiO_2/crosslinked carboxymethyl starch composite for high-efficiency adsorption and photodegradation of cationic golden yellow X-GL dye. *Environmental Science and Pollution Research* **26**(24), 24395–24406.

Guyo, U., Mhonyera, J. & Moyo, M. 2015 Pb (II) adsorption from aqueous solutions by raw and treated biomass of maize stover–a comparative study. *Process Safety and Environmental Protection* **93**, 192–200.

Guyo, U., Matewere, N., Matina, K., Nharingo, T. & Moyo, M. 2017 Fabrication of a sustainable maize stover-graft-methyl methacrylate biopolymer for remediation of methyl red contaminated wasters. *Sustainable Materials and Technologies* **13**, 9–17.

Heidari, H. & Razmi, H. 2012 Multi-response optimization of magnetic solid phase extraction based on carbon coated Fe_3O_4 nanoparticles using desirability function approach for the determination of the organophosphorus pesticides in aquatic samples by HPLC–UV. *Talanta* **99**, 13–21.

Hirunpraditkoon, S., Tunthong, N., Ruangchai, A. & Nuithitikul, K. 2011 Adsorption capacities of activated carbons prepared from bamboo by KOH activation. *International Journal of Chemical and Molecular Engineering* **5**(6), 491–495.

Ibrahim, M. B. 2013 Thermodynamics and adsorption efficiencies of maize cob and sawdust for the remediation of toxic metals from wastewater. *Journal of Geoscience and Environment Protection* **1**(2), 18–21.

Ismail, S. N. A. S., Rahman, W. A., Rahim, N. A. A., Masdar, N. D. & Kamal, M. L. 2018 Adsorption of malachite green dye from aqueous solution using corn cob. In *AIP Conference Proceedings*. AIP Publishing LLC, 17–18 April, 2018, Penang, Malaysia. https://doi.org/10.1063/1.5066992.

Ismail, M., Fadzil, M., Rosmadi, N., Razali, N. & Daud, A. M. 2019 Acid treated corn stalk adsorbent for removal of alizarin yellow dye in wastewater. In *Journal of Physics: Conference Series*. IOP Publishing, August, 2019, Penang Island, Malaysia.

Iwuozor, K. O., Akpomie, K. G., Conradie, J., Adegoke, K. A., Oyedotun, K. O., Ighalo, J. O., Amaku, J. F., Olisah, C. & Adeola, A. O. 2022a Aqueous phase adsorption of aromatic organoarsenic compounds: A review. *Journal of Water Process Engineering* **49**, 103059.

Iwuozor, K. O., Emenike, E. C., Aniagor, C. O., Iwuchukwu, F. U., Ibitogbe, E. M., Temitayo, O. B., Omuku, P. E. & Adeniyi, A. G. 2022b Removal of pollutants from aqueous media using cow dung-based adsorbents. *Current Research in Green and Sustainable Chemistry* **5**, 100300. https://doi.org/10.1016/j.crgsc.2022.100300.

Iwuozor, K. O., Oyekunle, I. P., Emenike, E. C., Okoye-Anigbogu, S. M., Ibitogbe, E. M., Elemile, O., Ighalo, J. O. & Adeniyi, A. G. 2022c An overview of equilibrium, kinetic and thermodynamic studies for the sequestration of Maxilon dyes. *Cleaner Materials* **6**, 100148. https://doi.org/10.1016/j.clema.2022.100148.

Jalil, A., Triwahyono, S., Yaakob, M., Azmi, Z., Sapawe, N., Kamarudin, N., Setiabudi, H., Jaafar, N., Sidik, S. & Adam, S. 2012 Utilization of bivalve shell-treated *Zea mays* L. (maize) husk leaf as a low-cost biosorbent for enhanced adsorption of malachite green. *Bioresource Technology* **120**, 218–224.

Jassim, A., Amlah, L., Ali, D. & Aljabar, A. 2012 Preparation and characterization of activated carbon from Iraqi apricot stones. *Canadian Journal on Chemical Engineering & Technology* **3**, 60–65.

Javed, I., Javed, T. & Khan, M. N. 2021 A characteristic study of *Zea mays* L.(sweet corn) cobs for synthetic dye degradation from aqueous media. *Water Science and Technology* **83**(1), 52–62.

Jawad, A. H., Mohammed, S. A., Mastuli, M. S. & Abdullah, M. F. 2018 Carbonization of corn (*Zea mays*) cob agricultural residue by one-step activation with sulfuric acid for methylene blue adsorption. *Desalination and Water Treatment* **118**(3), 342–351.

Jia, D. & Li, C. 2015 Adsorption of Pb (II) from aqueous solutions using corn straw. *Desalination and Water Treatment* **56**(1), 223–231.

Jothirani, R., Kumar, P. S., Saravanan, A., Narayan, A. S. & Dutta, A. 2016 Ultrasonic modified corn pith for the sequestration of dye from aqueous solution. *Journal of Industrial and Engineering Chemistry* **39**, 162–175.

Jun, T. Y., Arumugam, S. D., Latip, N. H. A., Abdullah, A. M. & Latif, P. A. 2010 Effect of activation temperature and heating duration on physical characteristics of activated carbon prepared from agriculture waste. *Environ. Asia* **3**, 143–148.

Kamarehie, B., Jafari, A., Ghaderpoori, M., Amin Karami, M., Mousavi, K. & Ghaderpoury, A. 2019 Catalytic ozonation process using PAC/γ-Fe_2O_3 to Alizarin Red S degradation from aqueous solutions: A batch study. *Chemical Engineering Communications* **206**(7), 898–908.

Kamusoko, R., Jingura, R. M., Parawira, W. & Chikwambi, Z. 2021 Strategies for valorization of crop residues into biofuels and other value-added products. *Biofuels, Bioproducts and Biorefining* **15**(6), 1950–1964.

Kang, C., Shang, D., Yang, T., Zhu, L., Liu, F., Wang, N. & Tian, T. 2018 Preparation of corn stalk-walnut shell mix-based activated carbon and its adsorption of malachite green. *Chemical Research in Chinese Universities* **34**(6), 1014–1019.

Khodaie, M., Ghasemi, N., Moradi, B. & Rahimi, M. 2013 Removal of methylene blue from wastewater by adsorption onto $zncl_2$ activated corn husk carbon equilibrium studies. *Journal of Chemistry* **2013**, 383985. https://doi.org/10.1155/2013/383985.

Langmuir, I. 1916 The constitution and fundamental properties of solids and liquids. Part I. Solids. *Journal of the American Chemical Society* **38**(11), 2221–2295.

Lara-Vásquez, E. J., Solache-Ríos, M. & Gutiérrez-Segura, E. 2016 Malachite green dye behaviors in the presence of biosorbents from maize (*Zea mays* L.), their Fe-Cu nanoparticles composites and Fe-Cu nanoparticles. *Journal of Environmental Chemical Engineering* **4**(2), 1594–1603.

Leelavathy, K., Nageshwaran, V. & Bharathi, M. 2015 Comparative Study on Commercial and Corn Cobs Activated Carbon for Removal of Congo Red Dye. In: *Applied Mechanics and Materials*. Trans Tech Publ. **787**, 233–237. https://doi.org/10.4028/www.scientific.net/AMM.787.233.

Li, Y., Xing, B., Wang, X., Wang, K., Zhu, L. & Wang, S. 2019a Nitrogen-doped hierarchical porous biochar derived from corn stalks for phenol-enhanced adsorption. *Energy & Fuels* **33**(12), 12459–12468.

Li, X., Lu, X., Yang, J., Ju, Z., Kang, Y., Xu, J. & Zhang, S. 2019b A facile ionic liquid approach to prepare cellulose-rich aerogels directly from corn stalks. *Green Chemistry* **21**(10), 2699–2708.

Lima, D. R., Klein, L. & Dotto, G. L. 2017 Application of ultrasound modified corn straw as adsorbent for malachite green removal from synthetic and real effluents. *Environmental Science and Pollution Research* **24**(26), 21484–21495.

Lima, D. R., Sellaoui, L., Klein, L., Reis, G. S., Lima, É. C. & Dotto, G. L. 2018 Physicochemical and thermodynamic study of malachite green adsorption on raw and modified corn straw. *The Canadian Journal of Chemical Engineering* **96**(3), 779–787.

Lin, G., Wang, S., Zhang, L., Hu, T., Peng, J., Cheng, S., Fu, L. & Srinivasakannan, C. 2018 Selective recovery of Au (III) from aqueous solutions using 2-aminothiazole functionalized corn bract as low-cost bioadsorbent. *Journal of Cleaner Production* **196**, 1007–1015.

Lin, G., Hu, T., Wang, S., Xie, T., Zhang, L., Cheng, S., Fu, L. & Xiong, C. 2019 Selective removal behavior and mechanism of trace Hg (II) using modified corn husk leaves. *Chemosphere* **225**, 65–72.

Liu, C.-M., Diao, Z.-H., Huo, W.-Y., Kong, L.-J. & Du, J.-J. 2018a Simultaneous removal of Cu2+ and bisphenol A by a novel biochar-supported zero valent iron from aqueous solution: Synthesis, reactivity and mechanism. *Environmental Pollution* **239**, 698–705.

Liu, S., Ge, H., Cheng, S. & Zou, Y. 2018b Green synthesis of magnetic 3D bio-adsorbent by corn straw core and chitosan for methylene blue removal. *Environmental Technology* **41**(16), 2109–2121. https://doi.org/10.1080/09593330.2018.1556345.

Liu, L., Li, Y. & Fan, S. 2019 Preparation of KOH and H_3PO_4 modified biochar and its application in methylene blue removal from aqueous solution. *Processes* **7**(12), 891.

Liu, Z., Sun, Y., Xu, X., Meng, X., Qu, J., Wang, Z., Liu, C. & Qu, B. 2020a Preparation, characterization and application of activated carbon from corn cob by KOH activation for removal of Hg (II) from aqueous solution. *Bioresource Technology* **306**, 123154.

Liu, S., Ge, H., Cheng, S. & Zou, Y. 2020b Green synthesis of magnetic 3D bio-adsorbent by corn straw core and chitosan for methylene blue removal. *Environmental Technology* **41**(16), 2109–2121.

Loya-González, D., Loredo-Cancino, M., Soto-Regalado, E., Rivas-García, P., de Jesús Cerino-Córdova, F., García-Reyes, R. B., Bustos-Martínez, D. & Estrada-Baltazar, A. 2019 Optimal activated carbon production from corn pericarp: A life cycle assessment approach. *Journal of Cleaner Production* **219**, 316–325.

Ma, F., Zhao, B. & Diao, J. 2016 Adsorption of cadmium by biochar produced from pyrolysis of corn stalk in aqueous solution. *Water Science and Technology* **74**(6), 1335–1345.

Ma, D., Zhu, B., Cao, B., Wang, J. & Zhang, J. 2017 Fabrication of the novel hydrogel based on waste corn stalk for removal of methylene blue dye from aqueous solution. *Applied Surface Science* **422**, 944–952.

Ma, H., Yang, J., Gao, X., Liu, Z., Liu, X. & Xu, Z. 2019 Removal of chromium (VI) from water by porous carbon derived from corn straw: Influencing factors, regeneration and mechanism. *Journal of Hazardous Materials* **369**, 550–560.

Maghri, I., Amegrissi, F., Elkouali, M., Kenz, A., Tanane, O., Talbi, M. & Salouhi, M. 2012 Comparison of adsorption of dye onto low-cost adsorbents. *Global Journal of Science Frontier Research Chemistry* **12**(4), 1–6.

Mahapatra, K., Ramteke, D. & Paliwal, L. 2012 Production of activated carbon from sludge of food processing industry under controlled pyrolysis and its application for methylene blue removal. *Journal of Analytical and Applied Pyrolysis* **95**, 79–86.

Malik, D., Jain, C., Yadav, A., Kothari, R. & Pathak, V. 2016 Removal of methylene blue dye in aqueous solution by agricultural waste. *International Journal of Engineering Research & Technology* **3**(7), 864–880.

Mallampati, R., Tan, K. S. & Valiyaveettil, S. 2015 Utilization of corn fibers and luffa peels for extraction of pollutants from water. *International Biodeterioration & Biodegradation* **103**, 8–15.

Maneechakr, P. & Karnjanakom, S. 2019 Environmental surface chemistries and adsorption behaviors of metal cations (Fe 3 +, Fe 2 +, Ca 2+ and Zn 2+) on manganese dioxide-modified green biochar. *RSC Advances* **9**(42), 24074–24086.

Manzoor, Q., Sajid, A., Hussain, T., Iqbal, M., Abbas, M. & Nisar, J. 2019 Efficiency of immobilized *Zea mays* biomass for the adsorption of chromium from simulated media and tannery wastewater. *Journal of Materials Research and Technology* **8**(1), 75–86.

Mbarki, F., Kesraoui, A., Seffen, M. & Ayrault, P. 2018 Kinetic, thermodynamic, and adsorption behavior of cationic and anionic dyes onto corn stigmata: Nonlinear and stochastic analyses. *Water, Air, & Soil Pollution* **229**(3), 1–17.

Medhat, A., El-Maghrabi, H. H., Abdelghany, A., Menem, N. M. A., Raynaud, P., Moustafa, Y. M., Elsayed, M. A. & Nada, A. A. 2021 Efficiently activated carbons from corn cob for methylene blue adsorption. *Applied Surface Science Advances* **3**, 100037.

Miraboutalebi, S. M., Nikouzad, S. K., Peydayesh, M., Allahgholi, N., Vafajoo, L. & McKay, G. 2017 Methylene blue adsorption via maize silk powder: Kinetic, equilibrium, thermodynamic studies and residual error analysis. *Process Safety and Environmental Protection* **106**, 191–202.

Mittal, H., Alhassan, S. M. & Ray, S. S. 2018 Efficient organic dye removal from wastewater by magnetic carbonaceous adsorbent prepared from corn starch. *Journal of Environmental Chemical Engineering* **6**(6), 7119–7131.

Mittal, H., Babu, R., Dabbawala, A. A. & Alhassan, S. M. 2020 Low-temperature synthesis of magnetic carbonaceous materials coated with nanosilica for rapid adsorption of methylene blue. *ACS Omega* **5**(11), 6100–6112.

Miyah, Y., Lahrichi, A. & Idrissi, M. 2016 Removal of cationic dye—Methylene blue—from aqueous solution by adsorption onto corn cob powder calcined. *Journal of Materials and Environmental Science* **7**(1), 96–104.

Mohanraj, J., Durgalakshmi, D., Balakumar, S., Aruna, P., Ganesan, S., Rajendran, S. & Naushad, M. 2020 Low cost and quick time absorption of organic dye pollutants under ambient condition using partially exfoliated graphite. *Journal of Water Process Engineering* **34**, 101078.

Moradi, O. & Sharma, G. 2021 Emerging novel polymeric adsorbents for removing dyes from wastewater: A comprehensive review and comparison with other adsorbents. *Environmental Research* **201**, 111534.

Mousavi, S. A., Zangeneh, H., Almasi, A., Nayeri, D., Monkaresi, M., Mahmoudi, A. & Darvishi, P. 2020 Decolourization of aqueous methylene blue solutions by corn stalk: Modeling and optimization. *Desalin. Water Treat.* **197**, 335–344.

Mousavi, S. A., Kamarehie, B., Almasi, A., Darvishmotevalli, M., Salari, M., Moradnia, M., Azimi, F., Ghaderpoori, M., Neyazi, Z. & Karami, M. A. 2021 Removal of Rhodamine B from aqueous solution by stalk corn activated carbon: Adsorption and kinetic study. *Biomass Conversion and Biorefinery* **13**, 7927–7936. https://doi.org/10.1007/s13399-021-01628-1.

Moyo, M., Chikazaza, L., Nyamunda, B. C. & Guyo, U. 2013 Adsorption batch studies on the removal of Pb (II) using maize tassel based activated carbon. *Journal of Chemistry* **2013**, 508934. https://doi.org/10.1155/2013/508934.

Mu, W., Bao, D., Chang, C. & Lian, F. 2020 Adsorption of Methyl Blue by Maize Waste Based Biochar: Adsorption Kinetics and Isotherms. In: *Journal of Physics: Conference Series*. IOP Publishing. 17–18 July, 2020, Shandong, China.

Muhammad, U. L., Zango, Z. U. & Kadir, H. A. 2019 Crystal violet removal from aqueous solution using corn stalk biosorbent. *Science World Journal* **14**(1), 133–138.

Muthusamy, P. & Murugan, S. 2016 Removal of lead ion using maize cob as a bioadsorbent. *International Journal of Engineering Research and Applications* **6**, 05–10.

Nadaroğlu, H., Lesani, A., Soleimani, S. S., Babagil, A. & Güngör, A. 2018 Efficient solar photocatalyst based on TiO_2/corn silk NPs composite for removal of a textile azo-dye from aqueous solution. *IIOAB J* **9**(4), 20–27.

Nethaji, S., Sivasamy, A. & Mandal, A. 2013 Preparation and characterization of corn cob activated carbon coated with nano-sized magnetite particles for the removal of Cr (VI). *Bioresource Technology* **134**, 94–100.

Noor, A. B. M. & Nawi, M. A. B. M. 2008 Textural characteristics of activated carbons prepared from oil palm shells activated with $zncl_2$ and pyrolysis under nitrogen and carbon dioxide. *Journal of Physical Science* **19**(2), 93–104.

Ogura, A. P., Lima, J. Z., Marques, J. P., Sousa, L. M., Rodrigues, V. G. S. & Espíndola, E. L. G. 2021 A review of pesticides sorption in biochar from maize, rice, and wheat residues: Current status and challenges for soil application. *Journal of Environmental Management* **300**, 113753.

Ohale, P. E., Igwegbe, C. A., Iwuozor, K. O., Emenike, E. C., Obi, C. C. & Białowiec, A. 2023 A review of the adsorption method for norfloxacin reduction from aqueous media. *MethodsX* **10**, 102180. https://doi.org/10.1016/j.mex.2023.102180.

Ojediran, J. O., Dada, A. O., Aniyi, S. O., David, R. O. & Adewumi, A. D. 2021 Mechanism and isotherm modeling of effective adsorption of malachite green as endocrine disruptive dye using acid functionalized maize cob (AFMC). *Scientific Reports* **11**(1), 21498.

Ojedokun, A. T. & Bello, O. S. 2017 Liquid phase adsorption of Congo red dye on functionalized corn cobs. *Journal of Dispersion Science and Technology* **38**(9), 1285–1294.

Okafor, J., Agbajelola, D., Peter, S., Adamu, M. & David, G. 2015 Studies on the adsorption of heavy metals in a paint industry effluent using activated maize cob. *Journal of Multidisciplinary Engineering Science and Technology* **2**(2), 39–46.

Olorundare, O., Msagati, T., Krause, R. W., Okonkwo, J. & Mamba, B. B. 2014 Steam activation, characterisation and adsorption studies of activated carbon from maize tassels. *Chemistry and Ecology* **30**(5), 473–490.

Omuku, P., Odidika, C., Ozukwe, A. & Iwuozor, K. 2022 A comparative evaluation of rain water obtained from corrugated roofing sheets within Awka Metropolis, Anambra State. *Iranian (Iranica) Journal of Energy & Environment* **13**(2), 134–140.

Ong, S. T., Gan, H. Y. & Leow, L. E. 2017 Utilization of corn cob and TiO_2 photocatalyst thin films for dyes removal. *Acta Chimica Slovenica* **64**(1), 144–158.

Örkün, Y., Karatepe, N. & Yavuz, R. 2012 Influence of temperature and impregnation ratio of H_3PO_4 on the production of activated carbon from hazelnut shell. *Acta Physica Polonica-Series A General Physics* **121**(1), 277.

Panneerselvam, P., Morad, N. & Tan, K. A. 2011 Magnetic nanoparticle (Fe_3O_4) impregnated onto tea waste for the removal of nickel (II) from aqueous solution. *Journal of Hazardous Materials* **186**(1), 160–168.

Paşka, O. M., Păcurariu, C. & Muntean, S. G. 2014 Kinetic and thermodynamic studies on methylene blue biosorption sing corn-husk. *Rsc Advances* **4**(107), 62621–62630.

Peng, D., Cheng, S., Li, H. & Guo, X. 2021 Effective multi-functional biosorbent derived from corn stalk pith for dyes and oils removal. *Chemosphere* **272**, 129963.

Petrović, M., Šoštarić, T., Stojanović, M., Milojković, J., Mihajlović, M., Stanojević, M. & Stanković, S. 2016 Removal of Pb2+ ions by raw corn silk (*Zea mays* L.) as a novel biosorbent. *Journal of the Taiwan Institute of Chemical Engineers* **58**, 407–416.

Petrović, M., Šoštarić, T., Stojanović, M., Petrović, J., Mihajlović, M., Ćosović, A. & Stanković, S. 2017 Mechanism of adsorption of Cu^{2+} and Zn^{2+} on the corn silk (*Zea mays* L.). *Ecological Engineering* **99**, 83–90.

Pezhhanfar, S. & Zarei, M. 2021 Introduction of maize cob and husk for wastewater treatment; evaluation of isotherms and artificial neural network modeling. *Journal of the Iranian Chemical Society* **19**, 231–246. https://doi.org/10.1007/s13738-021-02301-0.

Pezhhanfar, S. & Zarei, M. 2022 Introduction of maize cob and husk for wastewater treatment; evaluation of isotherms and artificial neural network modeling. *Journal of the Iranian Chemical Society* **19**, 231–246.

Ponce, J., da Silva Andrade, J. G., dos Santos, L. N., Bulla, M. K., Barros, B. C. B., Favaro, S. L., Hioka, N., Caetano, W. & Batistela, V. R. 2021 Alkali pretreated sugarcane bagasse, rice husk and corn husk wastes as lignocellulosic biosorbents for dyes. *Carbohydrate Polymer Technologies and Applications* **2**, 100061.

Qu, Y., Kang, S., Sun, J., Zhang, L., Sun, J., Yang, S. & Yang, J. 2020 Synthesis of graphene oxide/corn cob composites and investigation of their adsorption performance of dye. In: *Journal of Physics: Conference Series*. IOP Publishing. 1–3 May 2020, Zhuhai, China.

Ramamoorthy, M., Ragupathy, S., Sakthi, D., Arun, V. & Kannadasan, N. 2020 Synthesis of SnO_2 loaded on corn cob activated carbon for enhancing the photodegradation of methylene blue under sunlight irradiation. *Journal of Environmental Chemical Engineering* **8**(5), 104331.

Ranjbar, A., Heidarpour, M., Eslamian, S. & Shirvani, M. 2022 Investigating the performance of adsorbents made from the canola stalk for the removal of lead from aqueous solutions. *Arabian Journal of Geosciences* **15**(19), 1565.

Reddy, P. M. K., Verma, P. & Subrahmanyam, C. 2016 Bio-waste derived adsorbent material for methylene blue adsorption. *Journal of the Taiwan Institute of Chemical Engineers* **58**, 500–508.

Rehl, T., Lansche, J. & Müller, J. 2012 Life cycle assessment of energy generation from biogas – Attributional vs. consequential approach. *Renewable and Sustainable Energy Reviews* **16**(6), 3766–3775.

Ren, X., Wang, S., Jin, Y., Xu, D. & Yin, H. 2020 Adsorption properties of reactive dyes on the activated carbon from corn straw prepared by microwave pyrolysis. *Desalination and Water Treatment* **200**, 296–303.

Rosas-Castor, J. M., Garza-González, M. T., García-Reyes, R. B., Soto-Regalado, E., Cerino-Córdova, F. J., García-González, A. & Loredo-Medrano, J. A. 2014 Methylene blue biosorption by pericarp of corn, alfalfa, and agave bagasse wastes. *Environmental Technology* **35**(9), 1077–1090.

Sahoo, T. R. & Prelot, B. 2020 Adsorption processes for the removal of contaminants from wastewater: The perspective role of nanomaterials and nanotechnology. In: *Nanomaterials for the Detection and Removal of Wastewater Pollutants* (Barbara Bonelli, Francesca S. Freyria, Ilenia Rossetti, Rajandrea Sethi, eds). Elsevier, Amsterdam, Netherlands, pp. 161–222.

Sallau, A. B., Aliyu, S. & Ukuwa, S. 2012 Biosorption of chromium (VI) from aqueous solution by corn cob powder. *International Journal of Environment and Bioenergy* **4**(3), 131–140.

Sanghi, R. & Verma, P. 2013 Decolorisation of aqueous dye solutions by low-cost adsorbents: A review. *Coloration Technology* **129**(2), 85–108.

Saroj, S., Singh, S. V. & Mohan, D. 2015 Removal of colour (direct blue 199) from carpet industry wastewater using different biosorbents (maize cob, citrus peel and rice husk). *Arabian Journal for Science and Engineering* **40**(6), 1553–1564.

Sepúlveda, L. A., Cuevas, F. A. & Contreras, E. G. 2015 Valorization of agricultural wastes as dye adsorbents: Characterization and adsorption isotherms. *Environmental Technology* **36**(15), 1913–1923.

Sharma, A., Tomer, A., Singh, J. & Chhikara, B. S. 2019 Biosorption of metal toxicants and other water pollutants by corn (maize) plant: A comprehensive review. *Journal of Integrated Science and Technology* **7**(2), 19–28.

Solar, C., Sardella, F., Deiana, C., Lago, R. M., Vallone, A. & Sapag, K. 2008 Natural gas storage in microporous carbon obtained from waste of the olive oil production. *Materials Research* **11**, 409–414.

Soldatkina, L. & Yanar, M. 2021 Equilibrium, kinetic, and thermodynamic studies of cationic dyes adsorption on corn stalks modified by citric acid. *Colloids and Interfaces* **5**(4), 52.

Soldatkina, L. & Zavrichko, M. 2018 Equilibrium, kinetic, and thermodynamic studies of anionic dyes adsorption on corn stalks modified by cetylpyridinium bromide. *Colloids and Interfaces* **3**(1), 4.

Song, W., Gao, B., Zhang, T., Xu, X., Huang, X., Yu, H. & Yue, Q. 2015 High-capacity adsorption of dissolved hexavalent chromium using amine-functionalized magnetic corn stalk composites. *Bioresource Technology* **190**, 550–557.

Song, W., Gao, B., Xu, X., Xing, L., Han, S., Duan, P., Song, W. & Jia, R. 2016 Adsorption–desorption behavior of magnetic amine/Fe_3O_4 functionalized biopolymer resin towards anionic dyes from wastewater. *Bioresource Technology* **210**, 123–130.

Taha, N. A., Zattot, A. & Mohamed, E. 2021 Modification of corn stalk for high-performance adsorption of Coomassie Brilliant Blue dye in simulated polluted water: Kinetic study. *Global NEST Journal* **23**(2), 201–208.

Tan, K. A., Morad, N., Teng, T. T., Norli, I. & Panneerselvam, P. 2012 Removal of cationic dye by magnetic nanoparticle (Fe_3O_4) impregnated onto activated maize cob powder and kinetic study of dye waste adsorption. *APCBEE Procedia* **1**, 83–89.

Tan, X.-f., Liu, S.-b., Liu, Y.-g., Gu, Y.-l., Zeng, G.-m., Hu, X.-j., Wang, X., Liu, S.-h. & Jiang, L.-h. 2017 Biochar as potential sustainable precursors for activated carbon production: Multiple applications in environmental protection and energy storage. *Bioresource Technology* **227**, 359–372.

Tang, Y., Zhao, Y., Lin, T., Li, Y., Zhou, R. & Peng, Y. 2019 Adsorption performance and mechanism of methylene blue by H_3PO_4-modified corn stalks. *Journal of Environmental Chemical Engineering* **7**(6), 103398.

Tang, Y., Lin, T., Jiang, C., Zhao, Y. & Ai, S. 2021 Renewable adsorbents from carboxylate-modified agro-forestry residues for efficient removal of methylene blue dye. *Journal of Physics and Chemistry of Solids* **149**, 109811.

Tejada-Tovar, C., Villabona-Ortiz, A., Ortega-Toro, R., López-Génes, J. & Negrete-Palacio, A. 2021 Elimination of cadmium (II) in aqueaous solution using corn cob (*Zea mays*) in batch system: Adsorption kinetics and equilibrium. *Revista Mexicana de Ingeniería Química* **20**(2), 1059–1077.

Tsamo, C., Assabe, M., Argue, J. & Ihimbru, S. 2019 Discoloration of methylene blue and slaughter house wastewater using maize cob biochar produced using a constructed burning chamber: A comparative study. *Scientific African* **3**, e00078.

Umpuch, C. 2015 Removal of green 40 from aqueous solutions by adsorption using organo-corn straw. *Engineering and Applied Science Research* **42**(3), 250–257.

Umpuch, C. & Jutarat, B. 2013 Adsorption of organic dyes from aqueous solution by surfactant modified corn straw. *International Journal of Chemical Engineering and Applications* **4**(3), 134.

Velmurugan, P., Shim, J. & Oh, B.-T. 2016 Removal of anionic dye using amine-functionalized mesoporous hollow shells prepared from corn cob silica. *Research on Chemical Intermediates* **42**(6), 5937–5950.

Vicinisvarri, I., Kumar, S. S., Aimi, N., Norain, I. & Izza, N. 2014 Preparation and characterization of phosphoric acid activated carbon from *Canarium odontophyllum* (Dabai) nutshell for methylene blue adsorption. *Research Journal of Chemistry and Environment* **18**(2), 57–62.

Vučurović, V. M., Razmovski, R. N., Miljić, U. D. & Puškaš, V. S. 2014 Removal of cationic and anionic azo dyes from aqueous solutions by adsorption on maize stem tissue. *Journal of the Taiwan Institute of Chemical Engineers* **45**(4), 1700–1708.

Wan, D., Wu, L., Liu, Y., Zhao, H., Fu, J. & Xiao, S. 2018 Adsorption of low concentration perchlorate from aqueous solution onto modified cow dung biochar: effective utilization of cow dung, an agricultural waste. *Science of the Total Environment* **636**, 1396–1407.

Wang, J. & Guo, X. 2020 Adsorption kinetic models: Physical meanings, applications, and solving methods. *Journal of Hazardous Materials* **390**, 122156.

Wang, L. & Wang, A. 2008 Adsorption properties of Congo red from aqueous solution onto N, O-carboxymethyl-chitosan. *Bioresource Technology* **99**(5), 1403–1408.

Wang, J., Wu, F., Wang, M., Qiu, N., Liang, Y., Fang, S. & Jiang, X. 2010 Preparation of activated carbon from a renewable agricultural residue of pruning mulberry shoot. *African Journal of Biotechnology* **9**(19), 2762–2767.

Wang, J., Xu, W., Chen, L., Huang, X. & Liu, J. 2014 Preparation and evaluation of magnetic nanoparticles impregnated chitosan beads for arsenic removal from water. *Chemical Engineering Journal* **251**, 25–34.

Wang, H., Xu, X., Ren, Z. & Gao, B. 2016 Removal of phosphate and chromium (VI) from liquids by an amine-crosslinked nano-Fe_3O_4 biosorbent derived from corn straw. *RSC Advances* **6**(53), 47237–47248.

Wang, F., Dang, Y.-q., Tian, X., Harrington, S. & Ma, Y.-q. 2018 Fabrication of magnetic activated carbons from corn cobs using the pickle liquor from the surface treatment of iron and steel. *New Carbon Materials* **33**(4), 303–309.

Wen, X., Yan, C., Sun, N., Luo, T., Zhou, S. & Luo, W. 2018 A biomass cationic adsorbent prepared from corn stalk: Low-cost material and high adsorption capacity. *Journal of Polymers and the Environment* **26**(4), 1642–1651.

Wu, C., Song, M., Jin, B., Wu, Y. & Huang, Y. 2013 Effect of biomass addition on the surface and adsorption characterization of carbon-based adsorbents from sewage sludge. *Journal of Environmental Sciences* **25**(2), 405–412.

Wu, L., Sun, J. & Wu, M. 2017 Modified cellulose membrane prepared from corn stalk for adsorption of methyl blue. *Cellulose* **24**(12), 5625–5638.

Yagmur, E., Ozmak, M. & Aktas, Z. 2008 A novel method for production of activated carbon from waste tea by chemical activation with microwave energy. *Fuel* **87**(15–16), 3278–3285.

Yahya, M. A., Al-Qodah, Z. & Ngah, C. Z. 2015 Agricultural bio-waste materials as potential sustainable precursors used for activated carbon production: A review. *Renewable and Sustainable Energy Reviews* **46**, 218–235.

Yaneva, Z. L. & Georgieva, N. V. 2013 Removal of diazo dye from the aqueous phase by biosorption onto ball-milled maize cob (BMMC) biomass of *Zea mays*. *Macedonian Journal of Chemistry and Chemical Engineering* **32**(1), 133–149.

Yang, C.-h. 1998 Statistical mechanical study on the Freundlich isotherm equation. *Journal of Colloid and Interface Science* **208**(2), 379–387.

Yang, F., Zhang, S., Sun, Y., Cheng, K., Li, J. & Tsang, D. C. 2018 Fabrication and characterization of hydrophilic corn stalk biochar-supported nanoscale zero-valent iron composites for efficient metal removal. *Bioresource Technology* **265**, 490–497.

Zhang, J., Zhang, P., Zhang, S. & Zhou, Q. 2014 Comparative study on the adsorption of tartrazine and indigo carmine onto maize cob carbon. *Separation Science and Technology* **49**(6), 877–886.

Zhang, H., Chen, L., Lu, M., Li, J. & Han, L. 2016 A novel film–pore–surface diffusion model to explain the enhanced enzyme adsorption of corn stover pretreated by ultrafine grinding. *Biotechnology for Biofuels* **9**(1), 1–12.

Zhang, Z., Wang, G., Li, W., Zhang, L., Chen, T. & Ding, L. 2020 Degradation of methyl orange through hydroxyl radical generated by optically excited biochar: Performance and mechanism. *Colloids and Surfaces A: Physicochemical and Engineering Aspects* **601**, 125034.

Zhao, Y., Xia, Y., Yang, H., Wang, Y. & Zhao, M. 2014 Synthesis of glutamic acid-modified magnetic corn straw: Equilibrium and kinetic studies on methylene blue adsorption. *Desalination and Water Treatment* **52**(1–3), 199–207.

Zheng, L., Dang, Z., Yi, X. & Zhang, H. 2010 Equilibrium and kinetic studies of adsorption of Cd (II) from aqueous solution using modified corn stalk. *Journal of Hazardous Materials* **176**(1–3), 650–656.

Zhu, Z., Li, A., Zhong, S., Liu, F. & Zhang, Q. 2008 Preparation and characterization of polymer-based spherical activated carbons with tailored pore structure. *Journal of Applied Polymer Science* **109**(3), 1692–1698.

Zhul-quarnain, A., Iwuozor, K. O., Modupe, I., Gold, E. & Chidubem, E. E. 2018 Adsorption of malachite green dye using orange peel. *Journal of Biomaterials* **2**(2), 10. doi:10.11648/j.jb.20180202.12.

Zolgharnein, J., Choghaei, Z., Bagtash, M., Feshki, S., Rastgordani, M. & Zolgharnein, P. 2016 Nano-Fe_3O_4 and corn cover composite for removal of Alizarin Red S from aqueous solution: Characterization and optimization investigations. *Desalination and Water Treatment* **57**(57), 27672–27685.

First received 21 May 2023; accepted in revised form 13 November 2023. Available online 29 November 2023